Synthesis and Thermoelectric Properties of 2- and 2,8-Substituted Tetrathiotetracenes

Mary Robert Garrett,[a] María Jesús Durán-Peña,[a] William Lewis,[b] Kaspars Pudzs,[c] Janis Uzulis,[c] Igors Mihailovs,[c] Björk Tyril,[a] Jonathan Shine,[a] Emily F. Smith,[d] Martins Rutkis,*[c] and Simon Woodward*[a]

[a] GSK Carbon Neutral Laboratories for Sustainable Chemistry, Jubilee Campus, University of Nottingham, Nottingham NG7 2TU, United Kingdom.
[b] University Park Campus, University of Nottingham, Nottingham NG7 2RD, United Kingdom.
[c] Institute for Solid State Physics, University of Latvia, 8 Kengaraga Street, LV-1063 Riga, Latvia.
[d] Nanoscale and Microscale Research Centre (nmRC), School of Chemistry, University Park Campus, University of Nottingham, Nottingham NG7 2RD, United Kingdom.

Electronic Supporting Information

1. General Experimental Procedures

Chemical Synthesis: Reactions involving air-sensitive reagents were carried out under nitrogen atmospheres using flame-dried Schlenk apparatus. Reaction temperatures refer to those of external baths. In these studies the ambient temperature range was 19-28 ^{o}C. Dimethylformamide (DMF) was dried overnight with A4 molecular sieves and bubbled with nitrogen for 10 minutes before use. All other solvents (toluene and diethyl ether) were used as received from commercial suppliers. The tetracene starting materials were prepared by a literature route and used without further purification.[S1] Infrared spectra were recorded on a Bruker Alpha FT-IR spectrometer by attenuated total reflection (diamond-ATR) on solid films. Nuclear magnetic resonance spectra were recorded on a Bruker Ascend 500 (500.1 MHz) spectrometer. Chemical shifts are quoted in parts per million (ppm) and referenced to residual reference solvent peaks using values provided by the MestReNova processing software;[S2] coupling constants (*J*) are quoted in Hertz. Proton and ^{13}C NMR studies of **1**

were carried out as dilute (1-2 mM) CS_2 (Sigma-Aldrich, ≥99%) solutions, referenced to external DMSO-d_6. This commercial CS_2 has residual, solvent derived, signals at 5.03, 1.11-0.98, 0.83, 0.70-0.53, and -0.22 ppm in its ^{1}H NMR spectrum. In ^{13}C NMR spectra (124.7 MHz, DMSO-d_6) an intense signal at δ_C 192.1 ppm was observed due to CS_2.[S3] To allow ease of comparison with the chemical shifts of our previous synthesized tetreacenes, compounds **1a-h** have been named and numbered similarly.[S1] UV-Vis spectra were recorded on an Agilent Cary spectrophotometer as nominal 10^{-5} M dichloromethane solutions. Semi-quantitative log(ε) values are given as a guide to relative peak height, accurate quantification is complicated by slow kinetic dissolution/degredation of solutions of **1**. Mass spectrometry was performed using a Bruker MicroTOF or VG Micromass AutoSpec spectrometers using electrospray (ESI), electron impact (EI) or field desorption (FD) ionization modes; theoretical HRMS molecular weights were determined using ChemDraw software;[S4] for HRMS analyses deviations from expected values (dev.) are given in ppm. Elemental CH analyses were conducted on a CE-440 Elemental Analyzer; the observed %carbon vs. calculated ideal values were used to estimate tetrathiotetracene (**1**) purities.

Physical Electronic Measurements: Data were collected as previously described.[S5] In brief, four gold electrodes were deposited by thermal evaporation in vacuum (7×10^{-6} mbar) on to a glass substrate (ISOLAB microscope slides) that had been rigorously cleaned as described previoulsy.[S5] Thin films of the derivatives **1a-h** were then deposited using thermal evaporation under vacuum (7×10^{-6} mbar, source temperature 500 ± 20 K). Identical substrate temperatures (300 K) and tetrathiotetracene evaporation rates (45 ng cm^{-2} s^{-1}) were used for deposition of all substrates. The sample holder was equipped with a Peltier element and thermistor for temperature control. Samples of **1** doped with iodine were attained by postdeposition sample exposure to the saturated iodine vapor (generated from 99.999% I_2 – Aldrich product 229695) at 1 bar pressure at ambient temperatures (ca. 23 ^{o}C) as described previously.[S6] Seebeck coefficient (S_b) and electrical conductivity $\sigma_{(\text{in plane})}$ measurements were carried out using a custom built system consisting of a PTC10 Stanford Research Systems PTC10 Programmable Temperature Controller with two PTC440 TEC drivers and a PTC330K 4-channel K-type thermocouple card, a Keithley 2182A Digital Low Voltagemeter and a custom designed sample holder. All measurements were made in plane using sample configurations and procedures already defined.[S5,S6] Thin film morphology was studied by scanning electron microscopy using a Tescan Lyra 3 FEF-SEM × FIB with a 5 keV electron beam as described before.[S5] For detailed descriptions see Sections 6-10.

2. General preparation of tetrathiotetracenes (1)

Typically under nitrogen or argon atmospheres tetracene **2** (50.0 mg) and sulfur (14.2 eq) were added to a long (ca 100 mm), flame-dried Schlenk tube (diameter 12 mm) with stirbar and equipped with a septum. Deoxygenated dimethyl formamide was added (to give a nominal concentration of 0.15 M of the tetracene **2**) and the septum was replaced with a mineral oil bubbler and a very slow flow of argon (1 bubble per 1-3 sec) established to remove H_2S (**TOXIC! STENCH!**). The reaction was then heated to reflux (bath 150-158 ^{o}C) under nitrogen for the times indicated in Table 1 (main paper) during which the reaction mixture changed from an orange suspension, to dark brown, to a deep, purple or emerald-green color until no **2** remained. The reaction mixture was filtered hot

(>110 °C) onto Whatman glass microfiber GF/A[S7] on a 25 mm 3-piece (Hartley)[S7] filter under an agron flow and washed with toluene (4 x 2 mL, until the washings were very pale green) and Et_2O (4 x 2 mL) and sucked dry in dim light to provide dark green powders, typically in 70-99% yield and >90% purity. The reactions could be scaled up by at least a factor of 10 (20 × for **1a**) without significant yield reduction; a 75 mm Hartley[S7] filter was used on 0.5-1.0 g scales. The crude tetrathiotetracenes were heated under vacuum (0.2 mbar) for 1 h at 130-140 °C to remove traces of DMF and sulfur by sublimation (see Section 3). On small scales this was carried out in the apparatus shown in Figure S1, on a large scales Kugelrohr apparatus was more practical. Tetrathiotetracenes **1** were recovered from the non-sublimed portion in the boat (Kegelrohr bulb). Based on the carbon CHN analysis and weights of recovered sulfur derivatives purified this way were typically 88-99% pure.

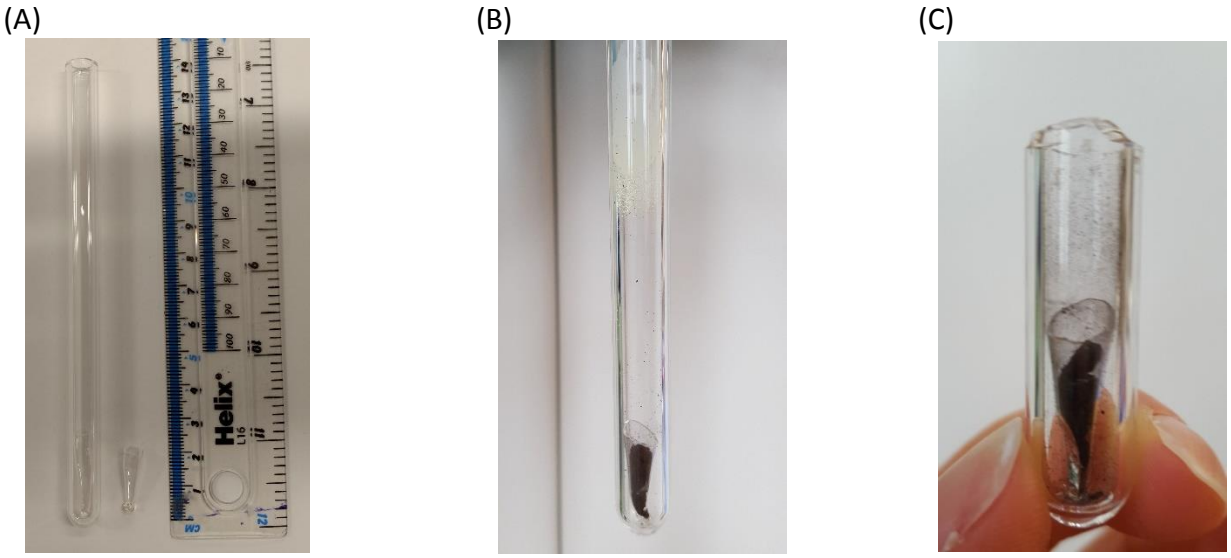

Fig. S1. (A) Small scale sublimation set up: tube and boat (loaded with ca. 15 mg of 1). (B) Post sublimation; the heated sand bath top had been ca. 5 mm above the top of the boat. The sublimed sulfur can be seen near the top of the pictured sublimation tube typically accounting for 0-7% w/w of the original mass of **1**. (c) Post tube-cut with remaining tetrathiotetracene (**CARE!** – tube was wrapped in electrical tape to mimimise 'sharp' injury potential during cutting and breaking).

Tetrathiotetracene (1a)

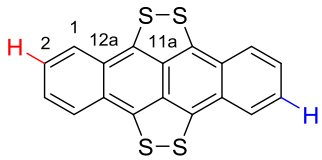

(**1a**)

Prepared using tetracene **2a** (116.9 mg, 0.51 mmol), sulfur (248.7 mg, 7.76 mmol) in DMF (3.4 mL) for 5 h to yield **1a** as a dark, green powder (156.1 mg, 0.44 mmol, 86%). Purification by sublimation of trace S_8 and solvents (130 °C, 0.2 mbar) out of the sample led to 95% pure **1a** at a cost of a 3% yield loss. **M.p.** >250 °C; **IR** (diamond-ATR): ν_{max}/cm^{-1} (pseudo emission 2165, 2032), 1611, 1516, 1384, 1362, 1316, 1302, 1247, 1236, 1146, 1010, 966, 942, 895, 833, 743, 714, 683, 449, 437; **^{1}H NMR** (500.1 MHz, CS_2, external DMSO-d_6 lock): δ 7.19-7.16 (m, 4H, H-1 or H-2), 7.14-7.09 (m, 4H, H-1 or H-2); **^{13}C NMR** (124.7 MHz, CS_2, external DMSO-d_6 lock): δ 134.7 (C), 132.3 (C), 125.3 (CH), 124.8 (CH), 124.4 (C); **UV/Vis** (CH_2Cl_2, 10^{-5} M): λ_{max}/nm 695 (log ε 5.0), 639 (log ε 4.9), 588sh (log ε 4.7), 470 (log ε 4.9); **MS** (+EI) 351 (M^+); **HRMS** calcd. for $C_{18}H_8S_4$ *m/z* 351.9509 (M), found *m/z* 351.9516 (M) (dev. = 1.9 ppm); **Anal:** Calcd. for $C_{18}H_8S_4$ C, 61.33; H, 2.29; found C, 58.43; H, 2.19% corresponding to 95% purity, based on the more sensitive %C analysis. The reaction

could be scale-up to gram quantities without yield loss. As far as we can determine only the ^{1}H spectrum (in toluene-d_8) of **1a** has been reported (see Ref. [2] in main paper), despite its common use in radical cation salt formation. Our IR[S8] and UV-vis[S9] data are within experimental error of literature reports. Known **1a** was prepared by identical methods to **1b-h** to allow a positive control in film property studies (vs. comparisons to the highly purified TTT (**1a**) we had used previously[S6]).

2-Methyltetrathiotetracene (1b)

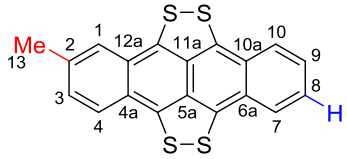

(**1b**)

Prepared using tetracene **2b** (300.0 mg, 1.24 mmol), sulfur (618.2 mg, 19.28 mmol) in DMF (8.5 mL) for 5.5 h to yield **1b** as a dark, green powder (391.0 mg, 1.07 mmol, 86%). Purification by sublimation of trace S_8 and solvents (130 ^{o}C, 0.2 mbar) out of the sample led to 96% pure **1a** at a cost of a 3% yield loss. **M.p.** >250 ^{o}C; **IR** (diamond-ATR): ν_{max}/cm^{-1} (pseudo emission 2220, 2013), 1623, 1608, 1318, 1303, 1235, 965, 850, 791, 738, 714, 686, 572, 450, 413; **UV/Vis** (CH_2Cl_2, 10^{-5} M): λ_{max}/nm 691 (log ε 5.1), 636 (log ε 5.0), 583sh (log ε 4.6), 470 (log ε 5.0), 377; **^{1}H NMR** (500.1 MHz, CS_2 external DMSO-d_6 lock) δ 7.18-7.16 (m, 2H, H-7/10 or H-8/9), 7.11 (d, *J* = 8.8 Hz, 1H, H-4), 7.06 (m, 2H, H-8/9 or H-7/10), 6.95 (app. s, 1H, H-1, the *meta* coupling was not resolved), 6.92 (app. d, *J* = 8.8 Hz, 1H, H-3, the *meta* coupling was not resolved); **^{13}C NMR** (124.7 MHz, CS_2, external DMSO-d_6 lock): δ 134.8(3) (C), 134.8 (C), 134.8 (C), 134.6 (C), 133.5 (C), 132.5 (C), 132.2 (C), 127.7 (CH), 125.5 (CH), 125.4 (CH), 125.3 (CH), 124.9 (CH), 124.8(5) (C), 124.8 (CH), 124.6 (C), 124.4 (C), 124.1 (CH), 123.2 (C), 21.8 (CH_3); **MS** (+EI) 366 (M^+); **HRMS** calcd. for $C_{19}H_{10}S_4$ *m/z* 365.9665 (M), found *m/z* 365.9660 (M) (dev. = -1.4 ppm); **Anal:** Calcd. for $C_{19}H_{10}S_4$ C, 62.26; H, 2.75; found C, 60.47; H, 2.63% coresponding to 96% purity. Only the low resolution mass spectrum of **1b** and a λ_{max} value (705 nm in 1,2,4-trichlorobenzene) have been reported in a patent.[S10]

2-Methoxytetrathiotetracene (1c)

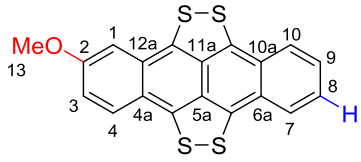

(**1c**)

Prepared using tetracene **2c** (49.6 mg, 0.19 mmol), sulfur (87.2 mg, 2.72 mmol) in DMF (1.3 mL) for 5 h to yield **1c** as a dark, green powder (58.7 mg, 0.15 mmol, 80%). Purification by sublimation of trace S_8 and solvents (130 ^{o}C, 0.2 mbar) out of the sample led to 88% pure **1a** at a cost of a 5% yield loss. **M.p.** >250 ^{o}C; **IR** (diamond-ATR): ν_{max}/cm^{-1} 2956, 2929, 2825, (pseudo emission 2151, 2022), 1625, 1608, 1529, 1475, 1430, 1323, 1302, 1236, 1209, 1181, 1154, 1029, 976, 933, 873, 806, 795, 763, 735, 685, 604, 573, 448; **UV/Vis** (CH_2Cl_2, 10^{-5} M): λ_{max}/nm 687 (log ε 4.8), 635 (log ε 4.7), 581sh (log ε 4.4), 468 (log ε 4.7); **^{1}H NMR** (500.1 MHz, CS_2 external DMSO-d_6 lock): δ 7.17-7.14 (m, 2H, H-7/10 or H8/9), 7.11 (d, *J* = 9.3 Hz, 1H, H-4), 7.07-7.02 (m, 2H, H-7/10 or H8/9), 6.75 (dd, *J* = 9.3, 2.2, Hz, 1H, H-3), 6.19 (d, *J* = 2.2 Hz, 1H, H-1); **^{13}C NMR** (124.7 MHz, CS_2, external DMSO-d_6 lock): δ 156.6 (C), 135.3 (C), 134.9 (C), 133.7 (C), 132.4 (C), 131.3 (C), 131.2 (C), 126.6 (CH), 125.3 (CH), 125.2 (C), 125.2 (CH), 124.8 (CH), 124.6 (C), 124.4 (CH), 124.0 (C), 120.8 (C), 120.1 (CH), 101.1 (CH), 54.4 (CH_3); **MS** (+EI) 382 (M^+); **HRMS** calcd. for $C_{19}H_{10}OS_4$ *m/z* 381.9614 (M), found *m/z* 381.9607 (M) (dev. = -1.8 ppm); **Anal:** Calcd. for $C_{19}H_{10}OS_4$ C, 59.66; H, 2.64; found C, 52.24; H, 1.14% corresponding to 88% purity. Only the ionization potential data for

1c has been reported.[S11] Solid samples of **1c** are rather suseptible to oxidative degredation (over 3 months) when stored in air under ambient conditions. The parent TTT **1a** is not overly affected in the same period; non alkoxy substituted **1** show intermediate behaviour. Storage of **1c**, and the other substituted tetracenes, at -20 °C under argon is recomended.

2-Phenyltetrathiotetracene (1d)

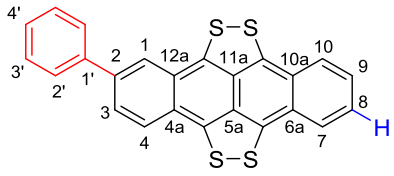

(**1d**)

Prepared using tetracene **2d** (292.4 mg, 0.96 mmol), sulfur (459.4 mg, 14.33 mmol) in DMF (6.6 mL) for 5 h to yield **1d** as a dark, green powder (411.7 mg, 0.96 mmol, >99%). Purification by sublimation of trace S_8 and solvents (130 °C, 0.2 mbar) out of the sample led to 96% pure **1a** at a cost of a 10% yield loss. **M.p.** >250 °C; **IR** (diamond-ATR): ν_{max}/cm^{-1} 3052, 3028, (pseudo emission 2115, 1991), 1609, 1528, 1466, 1447, 1400, 1363, 1320, 1303, 1249, 1225, 1151, 1134, 1075, 1036, 1001, 968, 941, 896, 860, 833, 811, 754, 742, 713, 683, 447; **UV/Vis** (CH_2Cl_2, 10^{-5} M): λ_{max}/nm 707 (log ε 4.5), 648 (log ε 4.3), 594sh (log ε 4.0), 482 (log ε 4.4); **^{1}H NMR** (500.1 MHz, CS_2 external DMSO-d_6 lock) δ 7.40-7.38 (m, 2H, H-2'), 7.33 (dd, *J* = 8.9, 1.6 Hz, 1H, H-3), 7.29 (app. s, 1H, H-1), 7.26 (d, *J* = 8.9 Hz, 1H, H-4), 7.21-7.16 (m, 4H, H-3' and H-7/10 or H-8/9), 7.11-7.09 (m, 1H, H-4') overlapped by 7.09-7.06 (m, 2H, H-7/10 or H-8/9); **^{13}C NMR** (124.7 MHz, CS_2, external DMSO-d_6 lock): δ 139.4 (C), 137.6 (C), 135.2 (C), 135.0 (C), 134.9 (2 × C overlap), 132.8 (C), 132.5 (C), 128.7 (CH), 127.6 (CH), 126.8 (CH), 126.0 (CH), 125.5 (CH), 125.1 (2 × CH overlap), 125.0 (2 × CH overlap), 124.9(9) (C), 124.7 (C), 124.6(6) (C), 123.7 (C), 122.9 (CH); the shifts of C8-10 are nearly coincident at ~124.8 ppm; **MS** (+EI) 428 (M); **HRMS** calcd. for $C_{24}H_{12}S_4$ *m/z* 427.9822 (M), found *m/z* 427.9820 (M) (dev. = <1 ppm); **Anal:** Calcd. for $C_{24}H_{12}S_4$ C, 67.26; H, 2.82; found C, 64.62; H, 2.59% corresponding to 96% purity.

2,8-Dimethyltetrathiotetracene (1e)

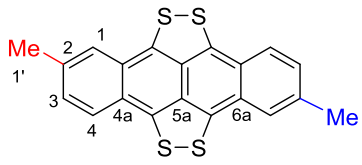

(**1e**)

Prepared using tetracene **2e** (47.7 mg, 0.19 mmol), sulfur (93.0 mg, 2.90 mmol) in DMF (1.3 mL) overnight to yield **1e** as a dark, green powder (63.2 mg, 0.17 mmol, 89%). Purification by sublimation of trace S_8 and solvents (130 °C, 0.2 mbar) out of the sample led to 98% pure **1a** at a cost of a 1% yield loss. **M.p.** >250 °C; **IR** (diamond-ATR): ν_{max}/cm^{-1} 2903, 2851, 2837, (pseudo emission 2169, 2023), 1620, 1321, 1305, 1233, 1222, 1185, 1142, 970, 903, 859, 789, 684, 563, 464; **UV/Vis** (CH_2Cl_2, 10^{-5} M): λ_{max}/nm 686 (log ε 5.2), 632 (log ε 5.1), 578sh (log ε 4.9), 469 (log ε 5.1); **^{1}H NMR** (500.1 MHz, CS_2 external DMSO-d_6 lock): δ 7.07 (d, *J* = 8.7 Hz, 2H, H-4), 6.91 (app. s, 2H, H-1, the small *meta* coupling was not resolved), 6.88 (app. d, *J* = 8.7 Hz, 2H, H-3, the small *meta* coupling was not resolved), 2.27 (s, 6H, H-1'); **^{13}C NMR** (124.7 MHz, CS_2, external DMSO-d_6 lock): δ 134.3(3) (C), 134.3(0) (C), 133.3 (C), 132.0 (C), 127.4 (CH), 125.0 (CH), 124.5 (C), 123.9 (CH), 123.0 (C), 21.6 (CH_3); **MS** (+EI) 380 (M); **HRMS** calcd. for $C_{20}H_{12}S_4$ *m/z* 379.9822 (M), found *m/z* 379.9820 (M) (dev. = <1 ppm); **Anal:** Calcd. for $C_{20}H_{12}S_4$ C, 63.12; H, 3.18; found C, 62.24; H, 3.2% corresponding to 99% purity.

2-Isopropyl-8-methylthiotetracene (1f)

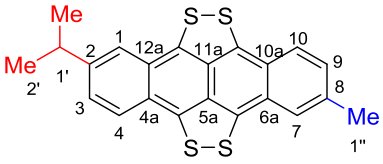

(**1f**)

Prepared using tetracene **2f** (52.4 mg, 0.18 mmol), sulfur (92.2 mg, 2.88 mmol) in DMF (1.2 mL) for overnight to yield **1f** as a dark, green powder (56.0 mg, 0.15 mmol, 74%). Purification by sublimation of trace S_8 and solvents (130 °C, 0.2 mbar) out of the sample led to 96% pure **1a** at a cost of a 2% yield loss. **M.p.** >250 °C; **IR** (diamond-ATR): ν_{max}/cm^{-1} 2953, 2929, (pseudo emission 2161, 2029), 1619, 1530, 1466, 1383, 1367, 1320, 1301, 1233, 1224, 1184, 1146, 1092, 976, 906, 854, 796, 684, 609, 451; **UV/Vis** (CH_2Cl_2, 10^{-5} M): λ_{max}/nm 684 (log ε 5.0), 631 (log ε 4.8), 578sh (log ε 4.6), 469 (log ε 4.9); **^{1}H NMR** (500.1 MHz, CS_2 external DMSO-d_6 lock): δ 7.10 (d, *J* = 8.8 Hz, 1H, H-10), 7.07 (d, *J* = 8.7 Hz, 1H, H-4), 6.96 (dd, *J* = 8.8, 1.7 Hz, 1H, H-9), 6.91 (app. s, 1H, H-7, the small *meta* coupling was not resolved), 6.88 (app. s, 1H, H-1, the small *meta* coupling was not resolved), overlapped by 6.88 (dd, *J* = 8.7, 1.3 Hz, 1H, H-3), 2.76 (hept, *J* = 6.9 Hz, 1H, H-1'), 2.26 (s, 3H, H-1"), 1.13 (d, *J* = 6.9 Hz, 6H, H-2"); **^{13}C NMR** (124.7 MHz, CS_2, external DMSO-d_6 lock): δ 144.8 (C), 134.3(5) (2 × C overlap), 134.3 (C), 134.1 (C), 133.7 (C), 133.3 (C), 132.0(5) (C), 132.0 (C), 127.4 (CH), 125.3 (CH), 125.1 (CH), 125.0(5) (CH), 124.5 (C), 123.4 (C), 123.9 (CH), 123.0 (C), 121.0 (CH), 34.2 (CH), 23.1 (CH_3), 21.6 (CH_3); **MS** (+EI) 408 (M); **HRMS** calcd. for $C_{22}H_{16}S_4$ *m/z* 408.0135 (M), found *m/z* 408.01228 (M) (dev. = 3 ppm); **Anal:** Calcd. for $C_{22}H_{16}S_4$, 64.67; H, 3.95; found C, 62.44; H, 3.52% corresponding to 96% purity.

2-Methoxy-8-methyltetrathiotetracene (1g)

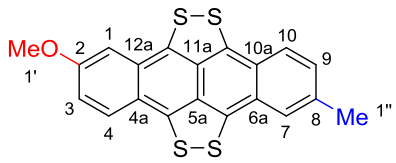

(**1g**)

Prepared using tetracene **2g** (57.0 mg, 0.21 mmol), sulfur (97.3 mg, 3.03 mmol) in DMF (3.0 mL) for overnight to yield **1g** as a dark, green powder (73.2 mg, 0.18 mmol, 88%). Purification by sublimation of trace S_8 and solvents (130 °C, 0.2 mbar) out of the sample led to 98% pure **1a** at a cost of a 3% yield loss. **M.p.** >250 °C; **IR** (diamond-ATR): ν_{max}/cm^{-1} 2893, 2877, (pseudo emission 2170, 2018), 1619, 1605, 1398, 1321, 1303, 1226, 1208, 1180, 1150, 1028, 976, 815, 779, 685, 639, 629, 500, 448; **UV/Vis** (CH_2Cl_2, 10^{-5} M): λ_{max}/nm 682 (log ε 5.1), 630 (log ε 5.0), 577sh (log ε 4.8), 467 (log ε 5.0); **^{1}H NMR** (500.1 MHz, CS_2 external DMSO-d_6 lock): δ 7.08 (d, *J* = 9.2 Hz, 1H, H-4), 7.07 (d, *J* = 8.8 Hz, 1H, H-10), 6.92 (app. s, 1H, H-7, the small *meta* coupling was not resolved), 6.89 (dd, *J* = 8.8, 1.5 Hz, 1H, H-9), 6.72 (dd, *J* = 9.3, 2.3 Hz, 1H, H-10), 6.17 (d, *J* = 2.3 Hz, 1H, H-1), 3.68 (s, 3H, H-1'), 2.27 (s, 3H, H-1''); **^{13}C NMR** (124.7 MHz, CS_2, external DMSO-d_6 lock): δ 156.4 (C), 135.0 (C), 134.1 (C), 133.6(2) (C), 133.5 (7) (C), 132.1 (C), 131.3 (C), 131.2 (C), 127.5 (CH), 126.5 (CH), 125.0(3) (C), 124.9(8) (CH), 124.3 (C), 123.9 (CH), 123.2 (C), 120.8 (C), 120.0 (CH), 101.1 (CH), 54.4 (CH_3), 21.6 (CH_3); **MS** (+EI) 396 (M); **HRMS** calcd. for $C_{20}H_{12}OS_4$ *m/z* 395.9771 (M), found *m/z* 395.97921 (M) (dev. = 5 ppm); **Anal:** Calcd. for $C_{20}H_{12}OS_4$ C, 60.58; H, 3.05; found C, 59.95; H, 2.94% corresponding to 98% purity. Solid samples of **1g** are suseptible to oxidative degredation (over 3 months) when stored in air under ambient conditions. The parent TTT **1a** is not overly affected in the same period, other derivatives of **1** show intermediate behavour. Storage of **1g** at -20 °C under argon is recomended. At partial reaction conversions (5 h vs. 18 h for complete conversion to **1g**) crystalline

2g could be recovered whose X-ray data is given in file CCDC 1811026 (via the Cambridge Crystallographic Data Centre: www.ccdc.cam.ac.uk).

2,8-Dimethoxytetrathiotetracene (1h)

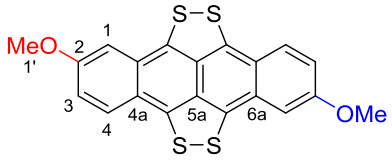

(**1h**)

Prepared using tetracene **2h** (54.3 mg, 0.19 mmol), sulfur (91.0 mg, 2.84 mmol) in DMF (4.2 mL) for 7d to yield **1h** as a dark, green powder (59.4 mg, 0.14 mmol, 75%). Purification by sublimation of trace S_8 and solvents (130 °C, 0.2 mbar) out of the sample led to 97% pure **1a** at a cost of a 4% yield loss. **M.p.** >250 °C; **IR** (diamond-ATR): ν_{max}/cm^{-1} 2830, (pseudo emission 2163, 2019), 1675, 1625, 1538, 1529, 1475, 1461, 1438, 1380, 1325, 1303, 1249, 1231, 1210, 1204, 1189, 1180, 1128, 1033, 983, 908, 831, 809, 795, 686, 604, 571, 465, 449; **UV/Vis** (CH_2Cl_2, 10^{-5} M): λ_{max}/nm 671 (log ε 4.7), 630 (log ε 4.6), 573sh (log ε 4.5), 464 (log ε 4.6); **^{1}H NMR** (500.1 MHz, CS_2 external DMSO-d_6 lock): δ 7.08 (d, *J* = 9.3 Hz, 2H, H-4), 6.73 (dd, *J* = 9.3, 2.4 Hz, 2H, H-3); 6.18 (d, *J* = 2.4 Hz, 2H, H-1), 3.68 (s, 3H, H-1'); **^{13}C NMR** (124.7 MHz, CS_2, external DMSO-d_6 lock): δ 126.5 (CH), 124.8 (C), 120.1 (CH), 101.1 (CH), 54.4 (CH_3), solubility issues meant that only one of the quaternary centres could be detected after 20000 scans; **MS** (+EI) 412 (M); **HRMS** calcd. for $C_{20}H_{12}O_2S_4$ *m/z* 411.9728 (M), found *m/z* 411.97264 (M) (dev. = <1 ppm); **Anal:** Calcd. for $C_{20}H_{12}O_2S_4$ C, 58.23; H, 2.93; found C, 56.40; H, 2.87% corresponding to 97% purity. In a separate run material of 88% purity was attained. Solid samples of **1h** are suseptible to oxidative degredation (over 3 months) when stored in air under ambient conditions. The parent TTT **1a** is not overly affected in the same period. Storage of **1h** at -20 °C under argon is recomended. If the sulfonation of **2h** was stopped at 24 h an insoluble black intermediate could be isolated by filtration. Assigned on the basis of ^{1}H NMR spectroscopy as the 1:1 adduct (**1h**·**2h**) **^{1}H NMR** (500.1 MHz, CS_2 external DMSO-d_6 lock): δ 8.11 (s, 2H, H-4 or H-12 of **2h**), 8.04 (s, 2H, H-4 or H-12 of **2h**), 7.52 (d, *J* = 9.2 Hz, 2H, H-4 of **2h**), 7.08 (d, *J* = 9.3 Hz, 2H, H-4 of **1h**), 6.78 (s plus unresolved long range couplings, 2H, H-1 of **2h**), 6.74 (app. dt *J* = 9.3, 2.4 Hz, 4H H-3 of **1h** and **2h**), 6.19 (d, *J* = 2.4 Hz, 2H, H-1 of **2h**), 3.70 (s, 6H, OMe of **1h**), 3.69 (s, 6H, OMe of **2h**). Attempts to sublime (250 °C, 0.1 mbar) (**1h**·**2h**) led to its separation into orange **2h** and green **1h**.

3. Representative preparation of tetrathiotetracenes (1) on gram scales

Under nitrogen tetracene **2a** (1.00 g, 4.38 mmol) and sulfur (1.99 g, 62.2 mmol, 14.2 equiv.) were added to a long, flame-dried Schlenk tube (ca. diameter 40 mm, height 240 mm) fitted with a stirbar and equipped with a rubber septum. Deoxygenated dimethyl formamide (28 mL) (to give a nominal concentration of 0.15 M in **2a**) was added and the septum was replaced with a mineral oil bubbler and a slow flow of nitrogen established to remove the H_2S that is emitted over the transformation (**CARE!** Toxic maloderous gas emitted). The reaction was then heated to reflux (>155 °C) under nitrogen for 16 h during which time the reaction mixture changed from an orange suspension, to an initial dark brown colour before becoming deep, emerald-green. The reaction mixture was filtered hot (>110 °C) onto Whatman glass microfiber GF/A[S4] paper using a 75 mm 3-piece Hartley[S4] filter, washed with toluene (4 x 5 mL) and Et_2O (4 x 5 mL) and sucked dry in dim light to provide a dark green powder (1.82 g). The crude tetrathiotetracene was heated, using a Kugelrohr apparatus, under vacuum (10 mbar) at 50 °C to remove traces of DMF and under higher vacuum (0.2 mbar) at

130 °C to remove traces of DMF and sulfur (that were trapped out at -78 °C). Tetrathiotetracene **1a** was recovered from the non-sublimed portion in the Kugelrohr bulb as a dark green powder (1.08 g, 3.07 mmol, 70%, typical range 69-99%). Based on the carbon CHN analysis and weights recovered, sulfur derivatives purified this way were 93±3% pure.

4. Optical properties of tetrathiotetracenes and parent tetracenes (2)

Comparisons of the optical properties of the tetrathiotetracenes **1** and their parent tetracenes **2** are given in **Table S1**.

Table S1. Optical band gap properties of the tetrathiotetracenes (**2**) compared to tetracenes (**1**).

		Tetrathiotetracenes			Tetracenes		
R^1	R^2	No.	λ_{max} (nm)	E_g(opt) (eV)	No.	λ_{max} (nm)	E_g(opt) (eV)
H	H	**1a**	695	1.53	**2a**	474	2.54
Me	H	**1b**	691	1.61	**2b**	476	2.51
MeO	H	**1c**	687	1.59	**2c**	482	2.46
Ph	H	**1d**	707	1.59	**2d**	483	2.48
Me	Me	**1e**	686	1.51	**2e**	476	2.50
*i*Pr	Me	**1f**	684	1.59	**2f**	475	2.49
MeO	Me	**1g**	682	1.54	**2g**	481	2.45
MeO	MeO	**1h**	671	1.62	**2h**	484	2.43

5. Representative ^{1}H and ^{13}C NMR spectra of prepared compounds

Partial ^{1}H and ^{13}C NMR spectra of tetrathiotetracenes are displayed on pages 9-16. Only aromatic regions are shown as the non spectroscopic grade CS_2 lead to the observation of solvent impurities in the aliphatic regions of the spectra that are only associated with the solvent.

Partial ^{1}H NMR and ^{13}C NMR spectra for the aromatic region of 1a (500.1 and 124.7 MHz respectively)

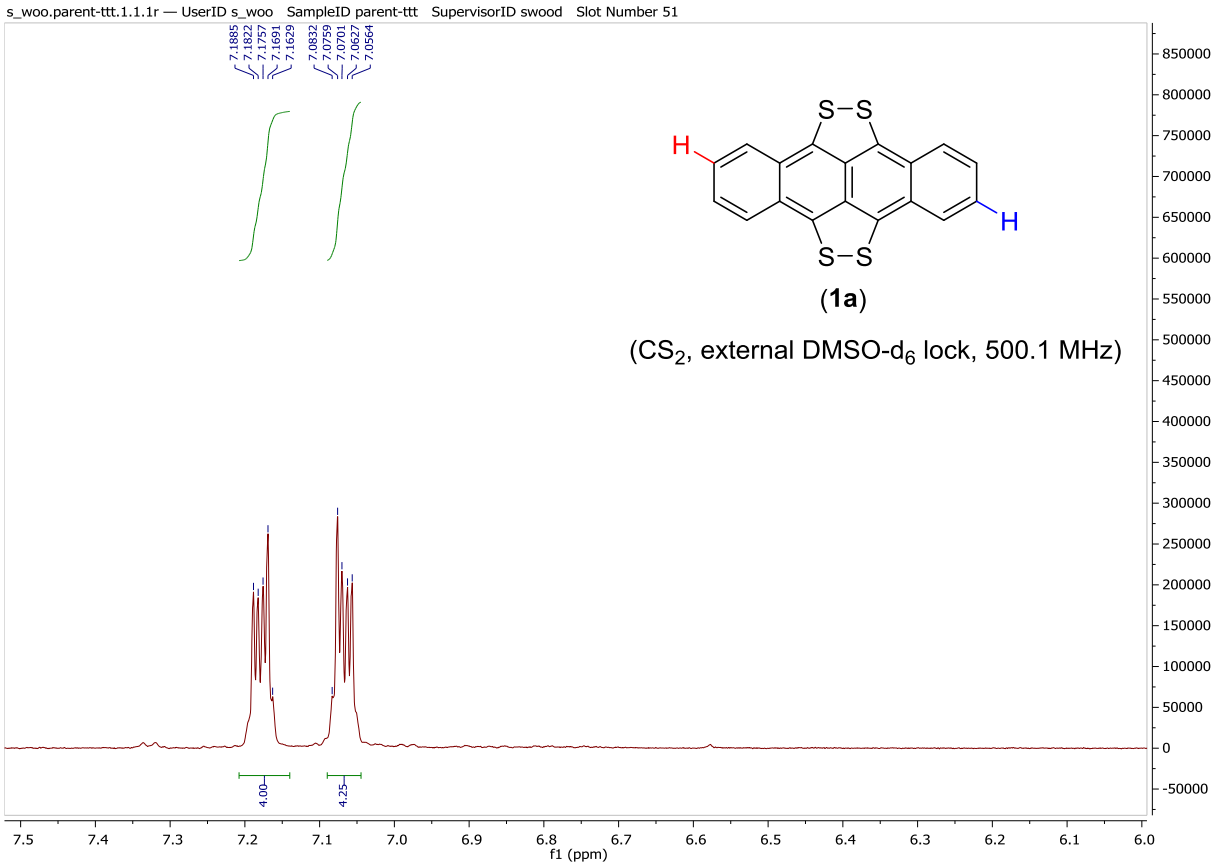

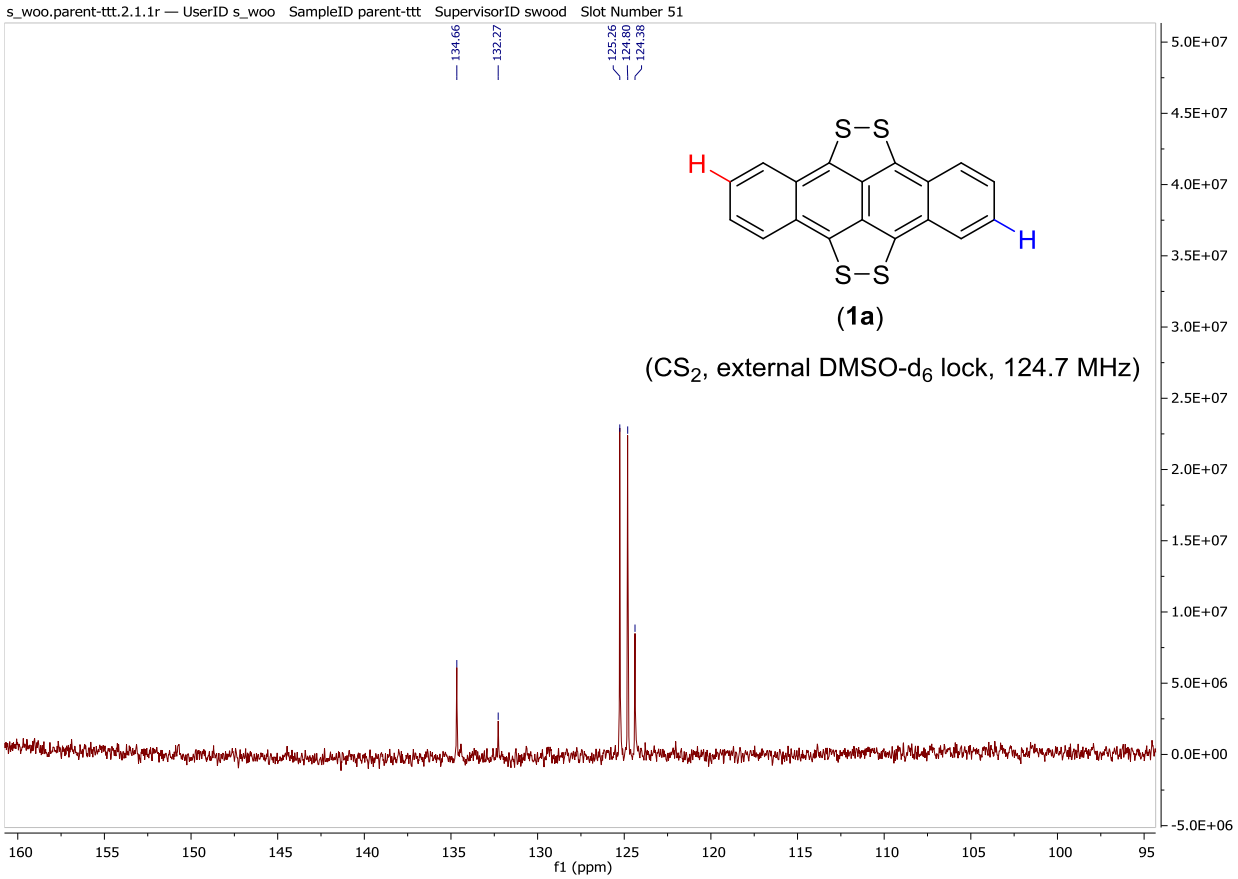

Partial ^{1}H NMR and ^{13}C NMR spectra for the aromatic region of 1b (500.1 and 124.7 MHz respectively)

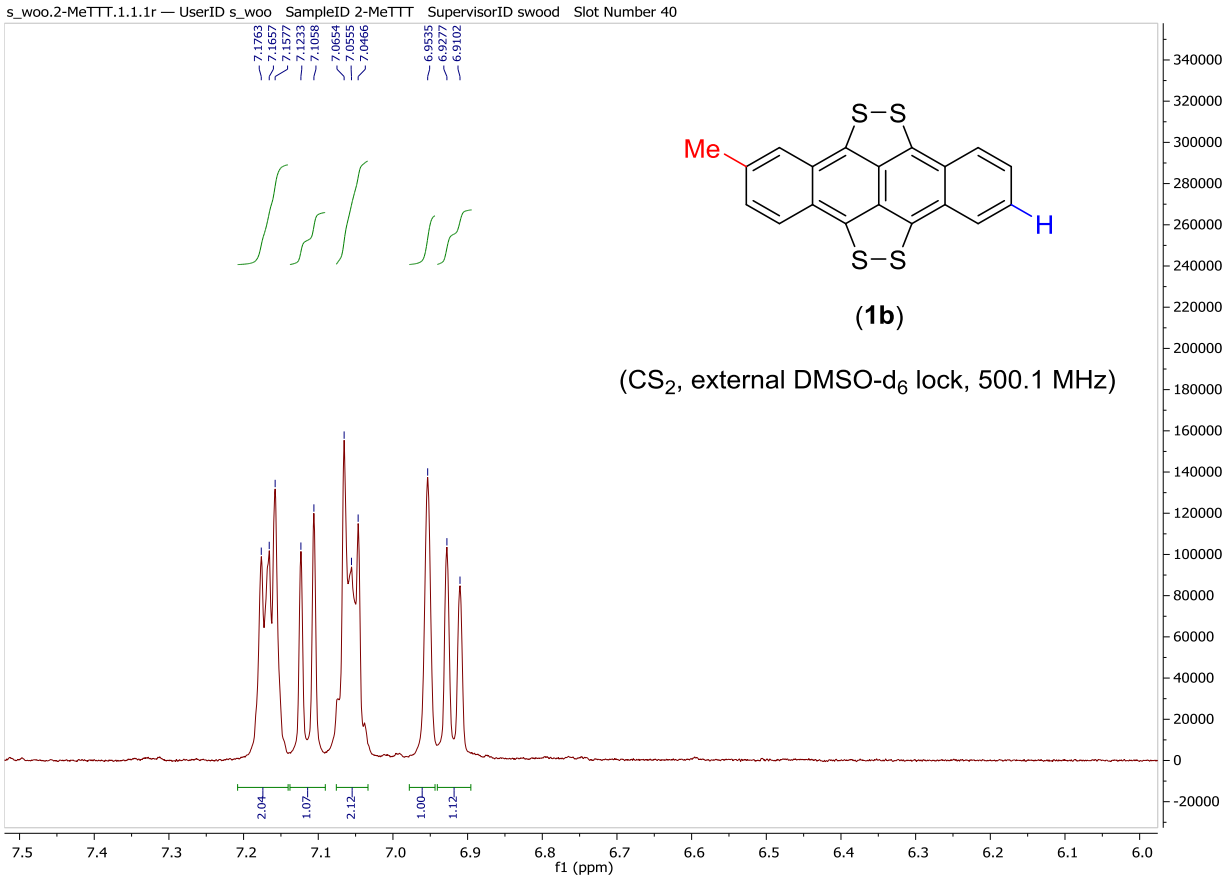

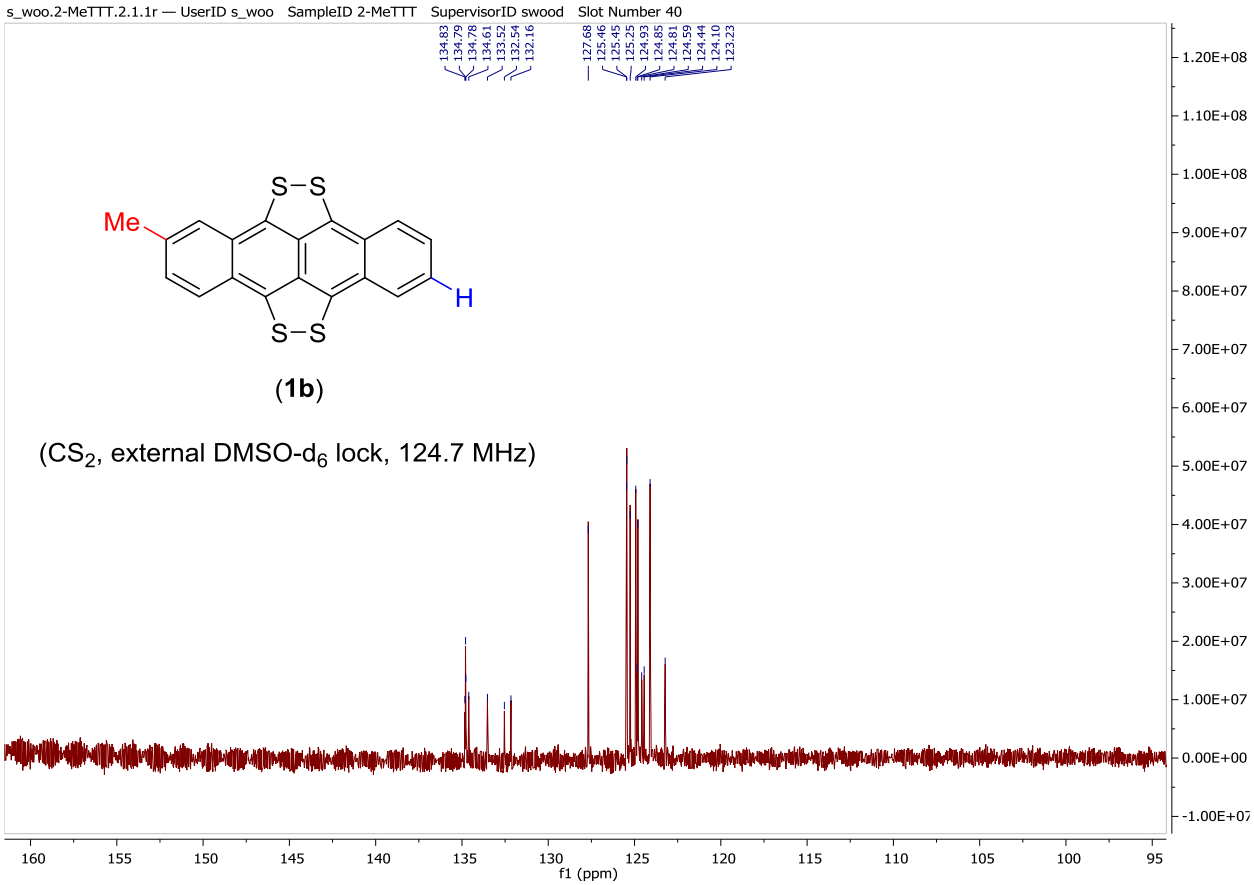

Partial ^{1}H NMR and ^{13}C NMR spectra for the aromatic region of 1c (500.1 and 124.7 MHz respectively)

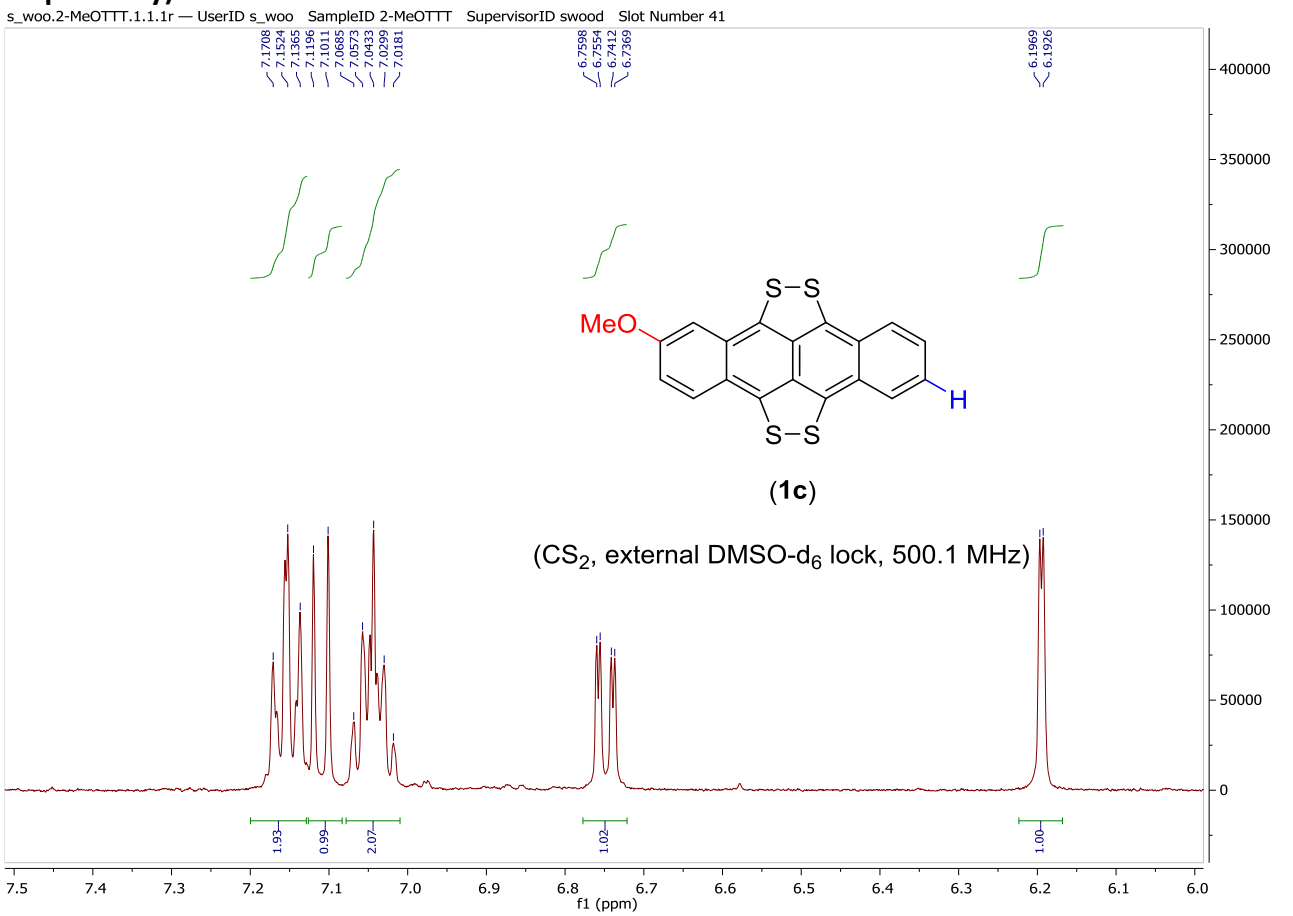

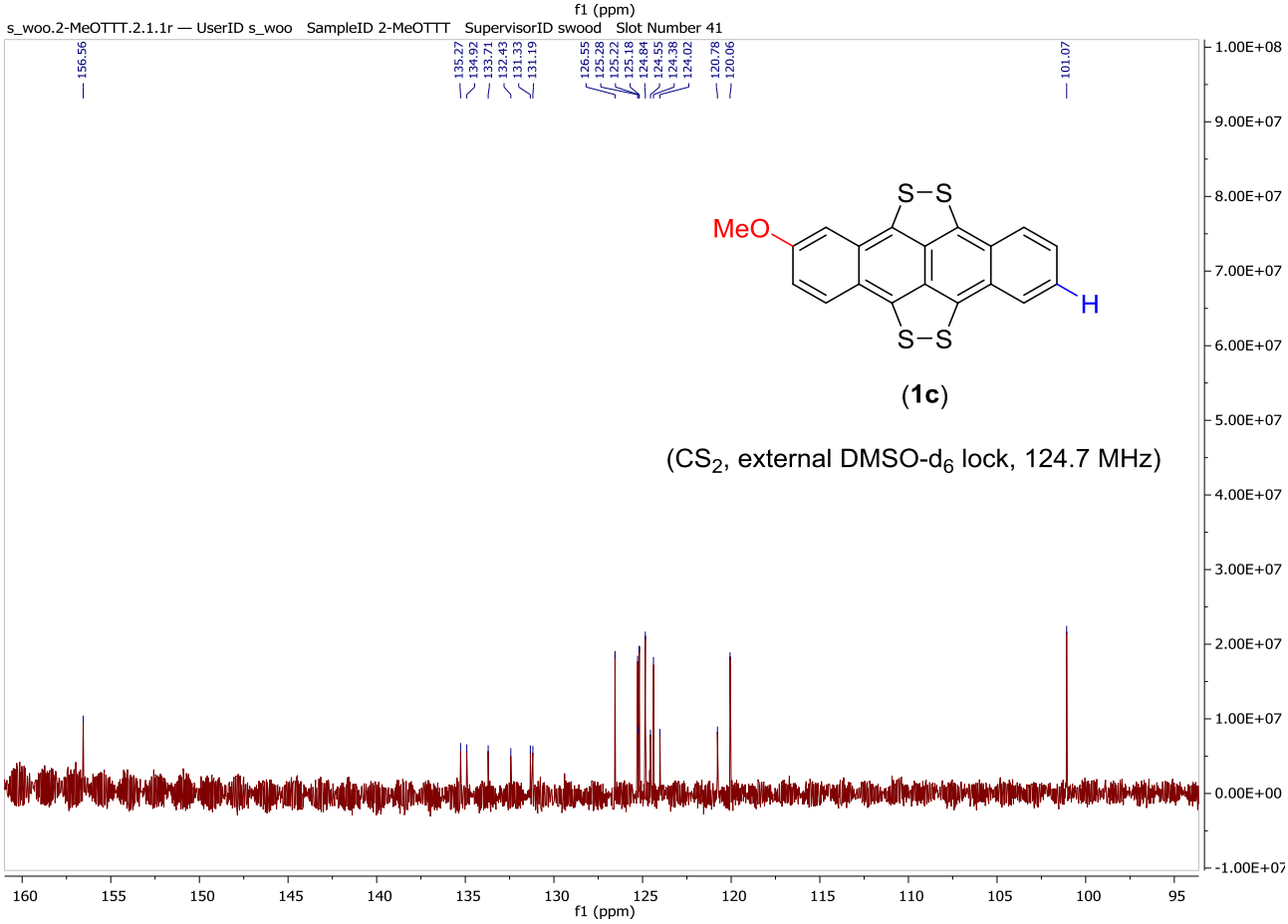

Partial ^{1}H NMR and ^{13}C NMR spectra for the aromatic region of 1d (500.1 and 124.7 MHz respectively)

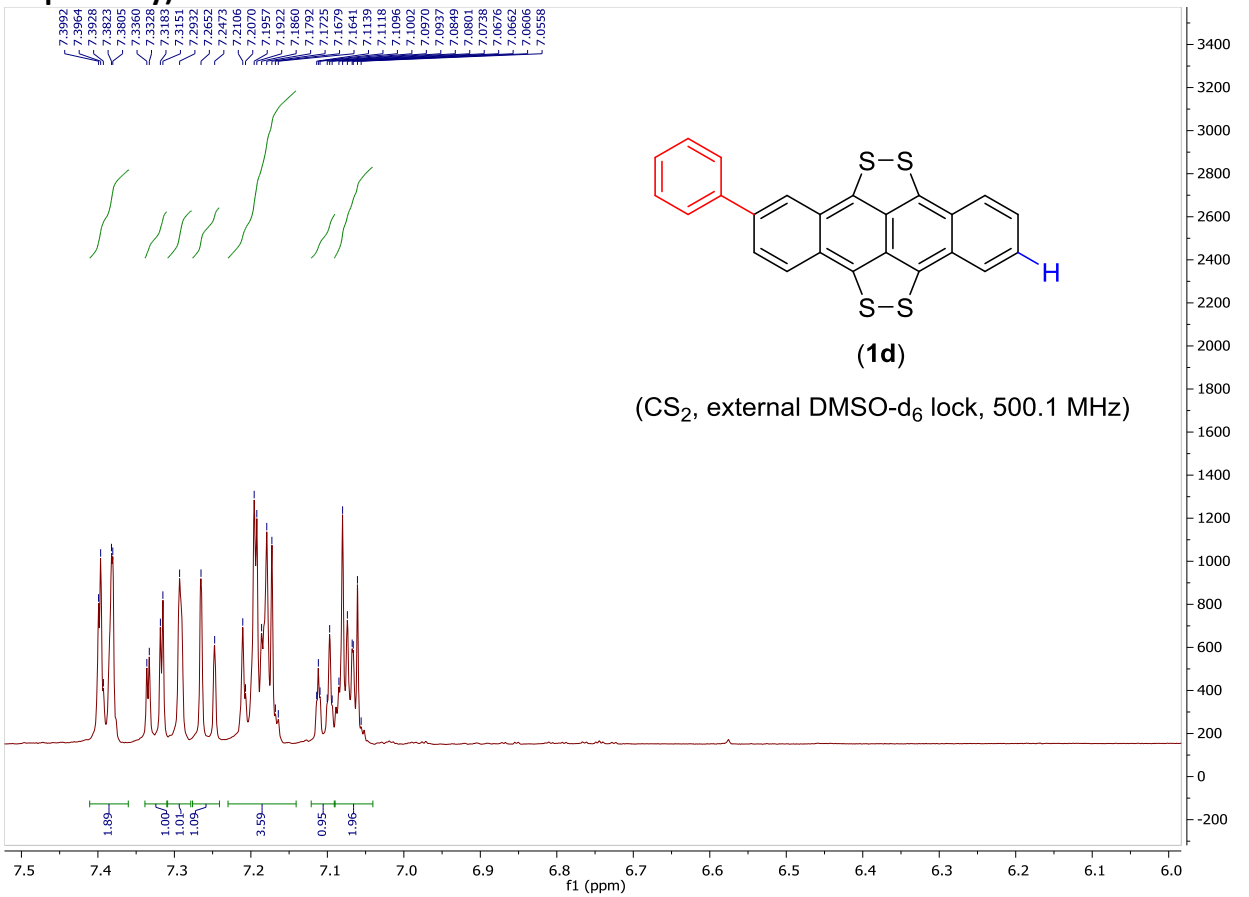

s_woo.ph-ttt.2.1.1r — UserID s_woo SampleID ph-ttt SupervisorID swood Slot Number 4

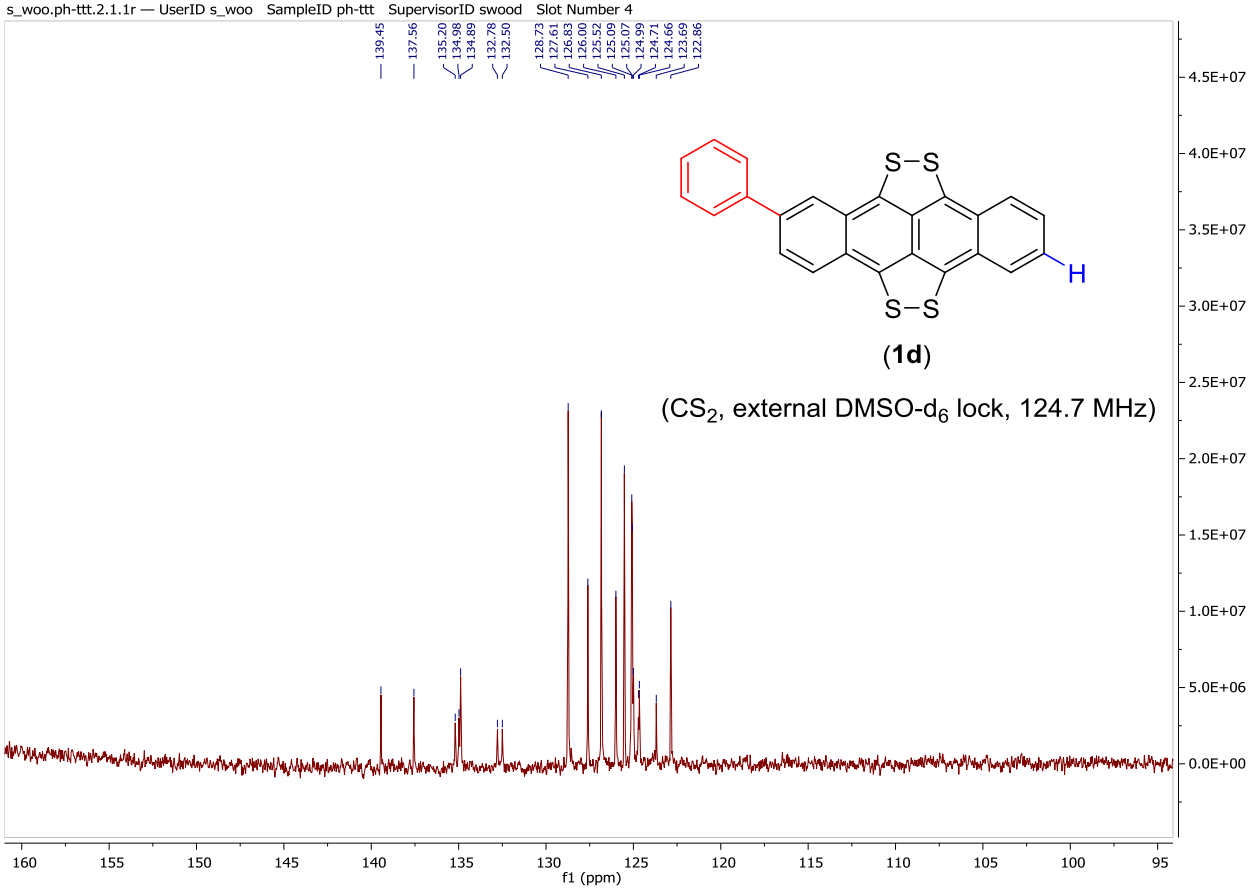

Partial ^{1}H NMR and ^{13}C NMR spectra for the aromatic region of 1e (500.1 and 124.7 MHz respectively)

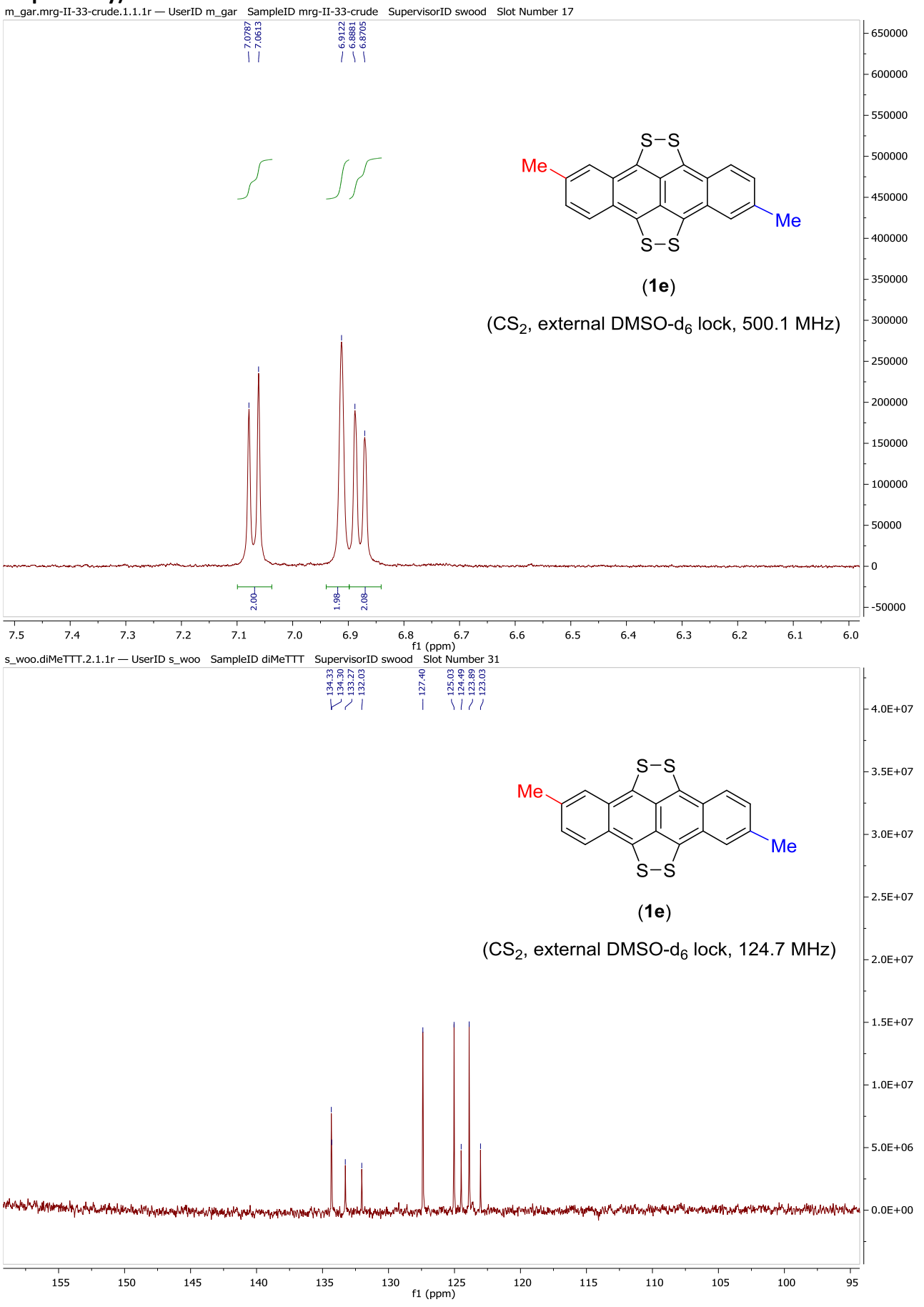

Partial ^{1}H NMR and ^{13}C NMR spectra for the aromatic region of 1f (500.1 and 124.7 MHz respectively)

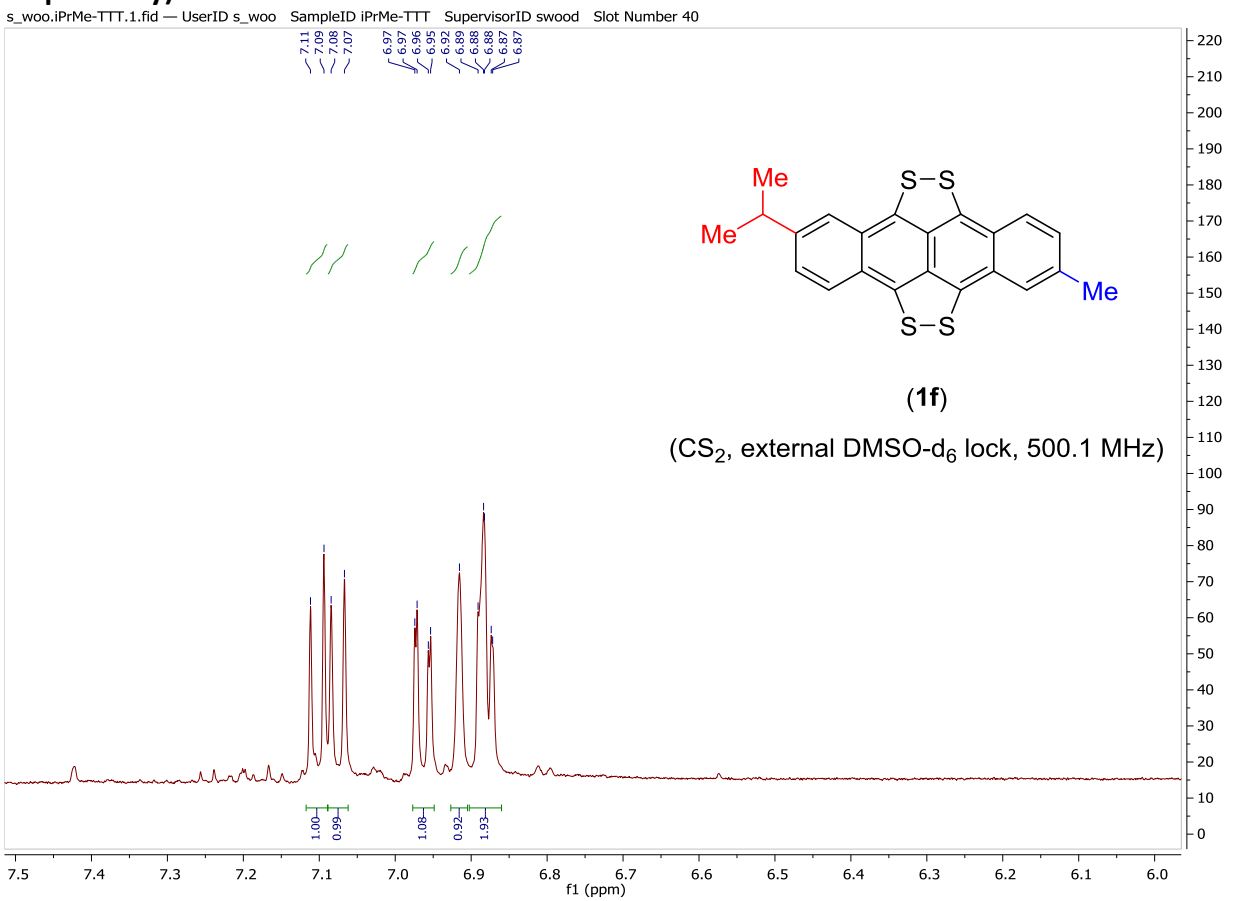

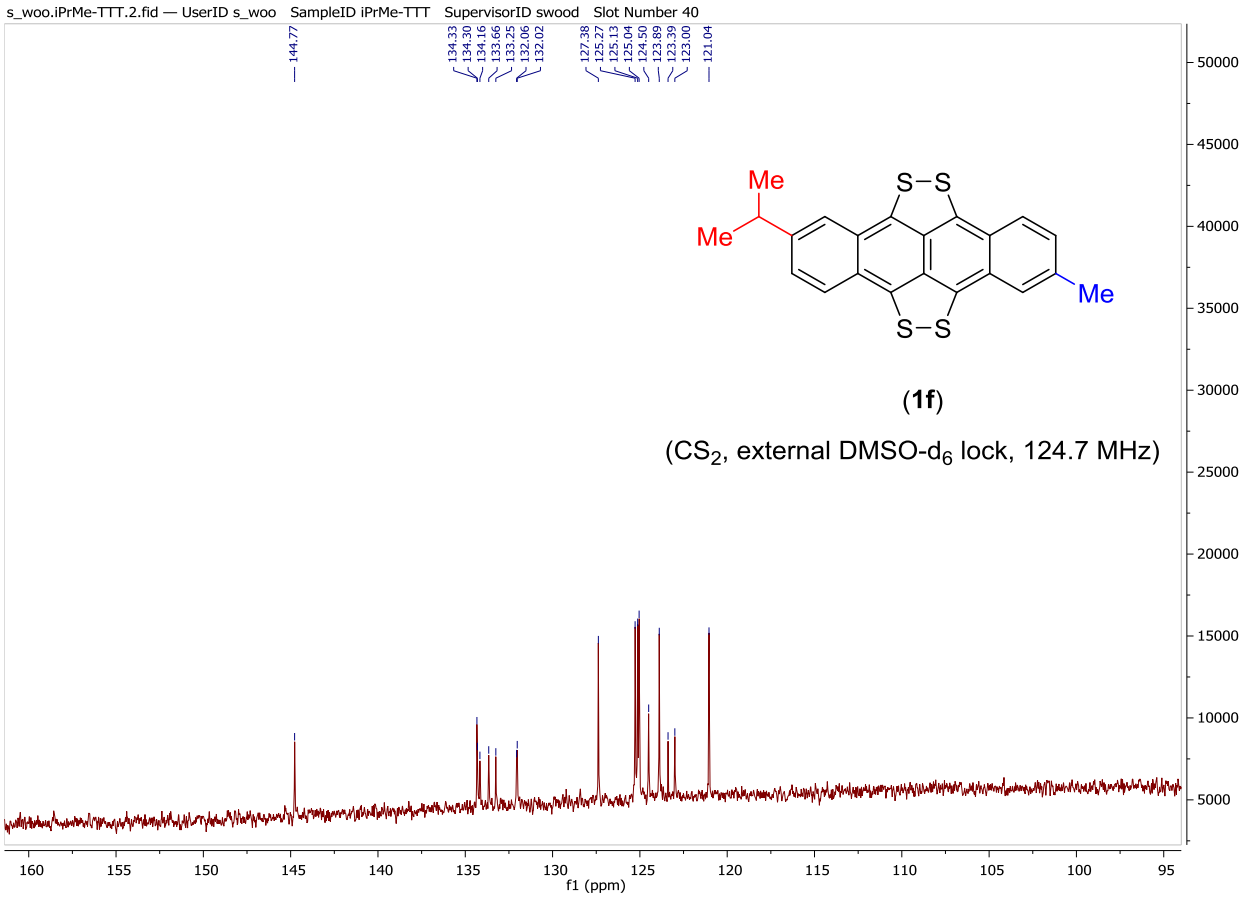

Partial ^{1}H NMR and ^{13}C NMR spectra for the aromatic region of 1g (500.1 and 124.7 MHz respectively)

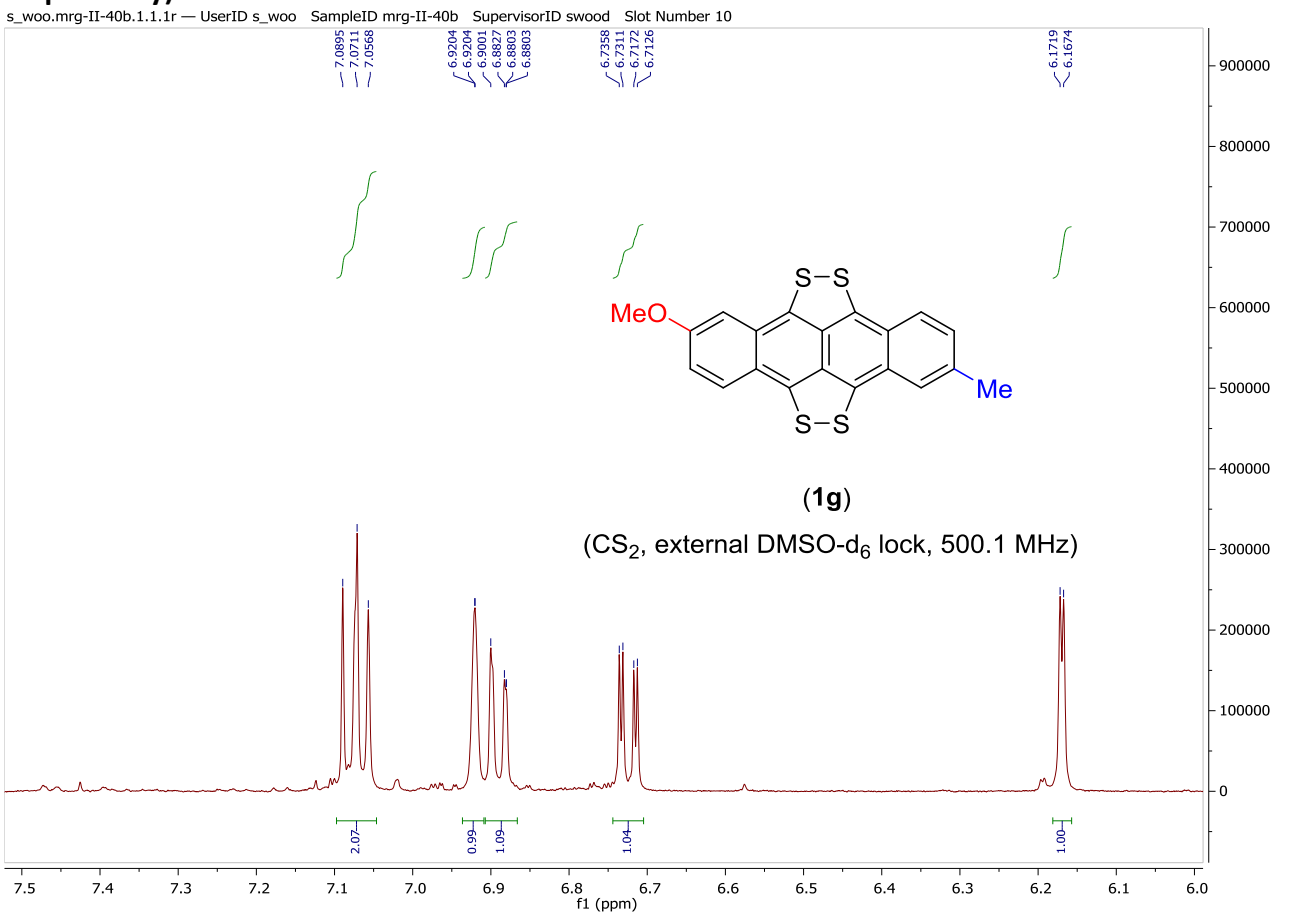

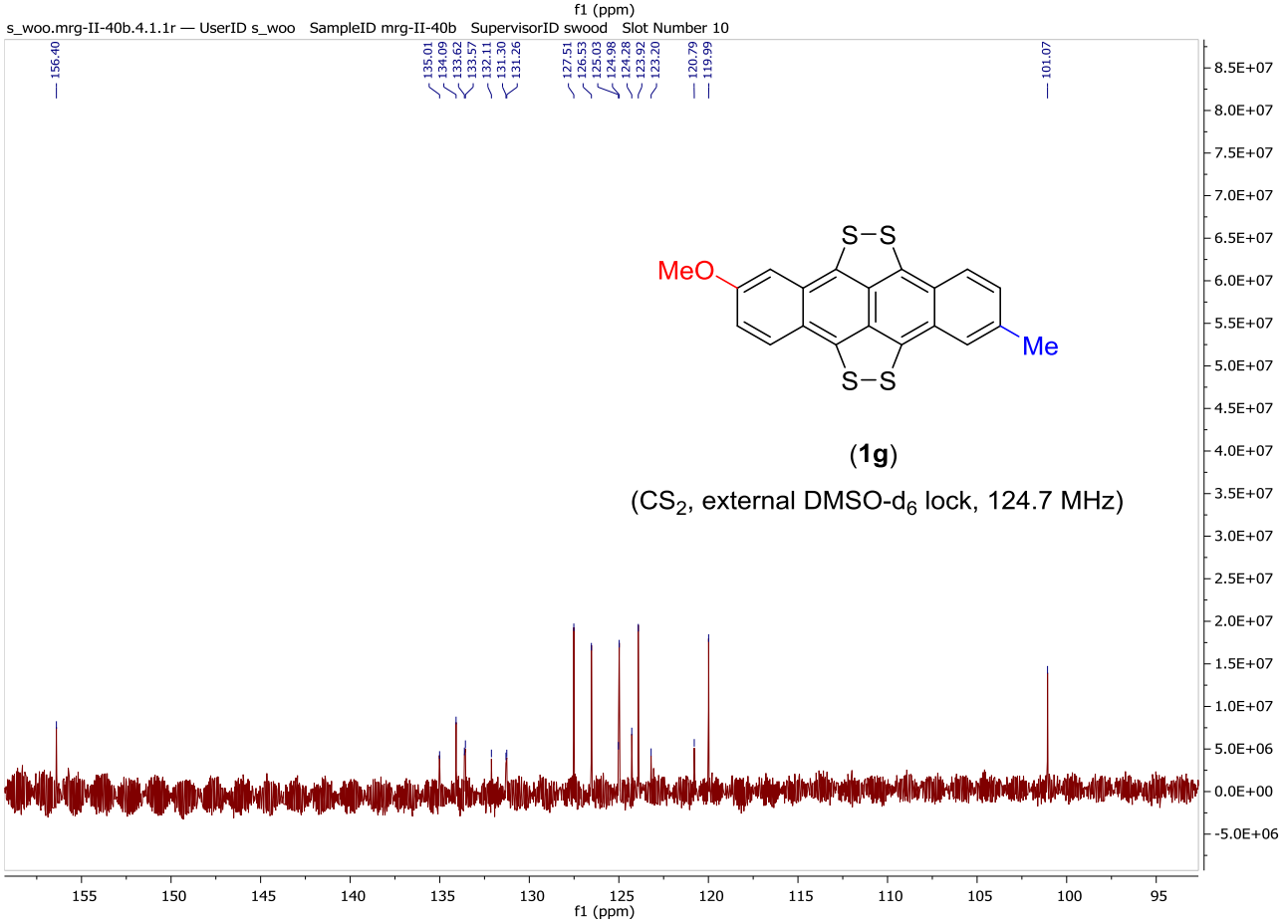

Partial ^{1}H NMR and ^{13}C NMR spectra for the aromatic region of 1h (500.1 and 124.7 MHz respectively)

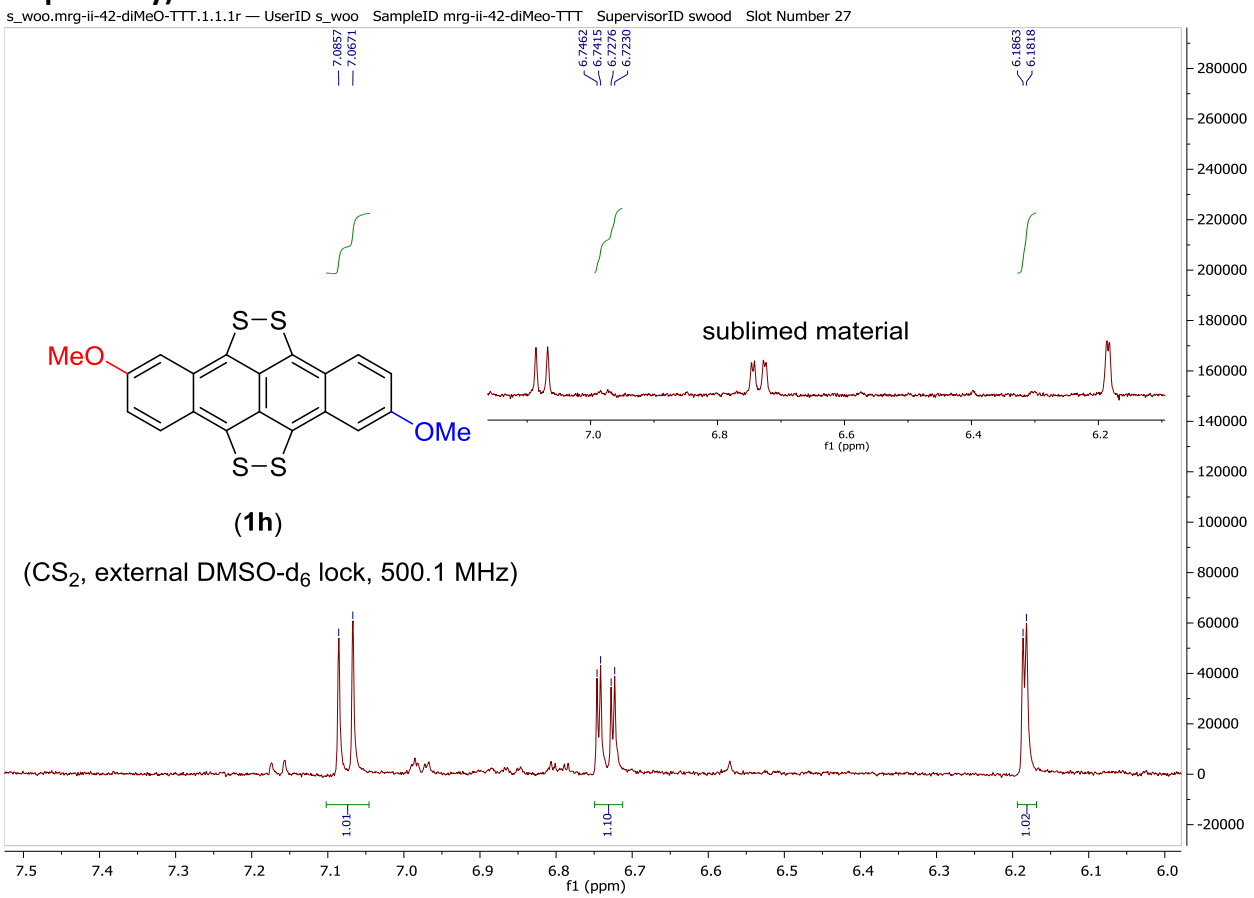

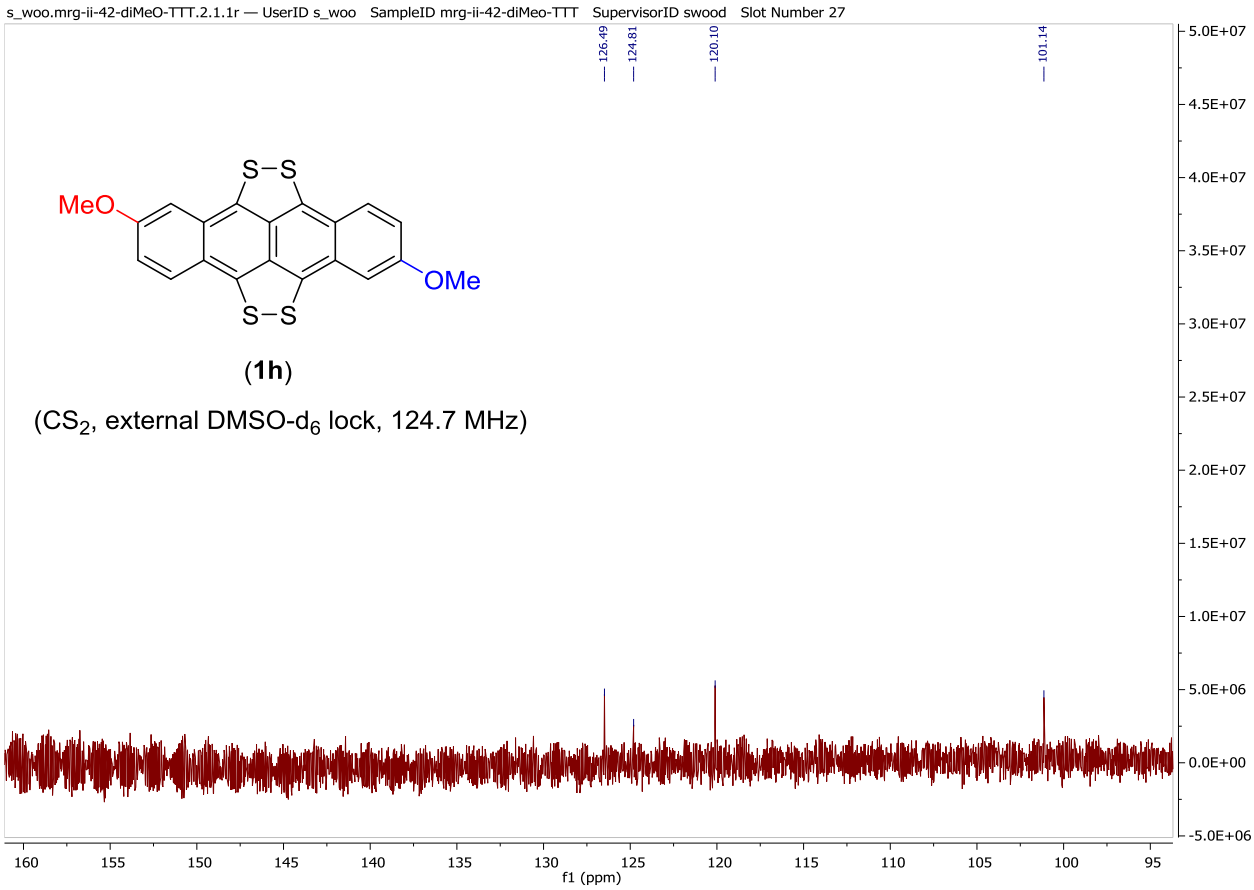

6. Deposition of thin films of 1 and their characterisation

Film deposition. Basal substrates (ISOLAB microscope slides) were cleaned sequentially with: chloroform, acetone, deionized water, Helmanex III detergent (2% v/v), deionized water and finally isopropanol using 15 min cycles in an ultrasonic bath. After cleaning the substrate was placed in our previously described apparatus.[S5] Four gold electrodes were deposited on to the substrate thermally (at 7×10^{-6} mbar) using masking techniques. The substrate was shuttered from samples of **1a-h** (10-20 mg at a distance of 100 mm) which were heated gradually to 500±20 K under 7×10^{-6} mbar vacuum until a sufficient deposition rate was attained (*ca*. 15 min was required). After *ca*. 15 min the shutter was opened and **1a-h** deposited at 45 ng cm^{-2} s^{-1} on to the substrate (whose temperature was 300 K). Control experiments confirmed this led to deposition of only pure **1** (≥99%) and excluded sulfur, volatile organics and dithiotetracene impurities. Films of 0.53 to 2.89 μm were attained, as measured by a Dektak 150 profilometer using stylus with diameter 12.5 μm and stylus force 0.1 mg. Representative films of **1** were subsequently removed from the apparatus and characterised by a 4-probe method for electrical conductivity, Seebeck coefficient measurements, SEM (using a Tescan Lyra 3 FEF-SEM × FIB with a 5 keV electron beam; this Section, Figure S3), photoemission yield spectroscopy (PYS, using an ENERGETIQ Laser Driven Light Source; Section 7, Figure S4), X-ray photoelectron spectroscopy (XPS, A Kratos Axis Ultra; Section 9, Figure SX). Samples of **1** (doped or undoped) were stable in air for at least 5 hours, as tested by re-assay by ATR-IR and the above techniques. Seebeck coefficient (S_b) and electrical conductivity measurements were carried out in air using a custom built system consisting of a PTC10 Stanford Research Systems PTC10 Programmable Temperature Controller with two PTC440 TEC drivers and a PTC330K 4-channel K-type thermocouple card, a Keithley 2182A Digital Low Voltagemeter, Keithley 6487 picoampermeter, Keithley 6514 electrometer, and a custom designed sample holder. All measurements were made in plane using sample configurations and procedures already defined.[S5,S6] Reproducibility across duplicate samples and remeasurements was determined to by ±10% for both $\sigma_{(in\text{-}plane)}$ and S_b experimentally. A temperature difference of 10 degees, with the cold side at 305 K and the hot side at 315 K, was used for S_b measurements. Preparation and characteration of iodine doped films of **1** are described in Sections 8-9.

Control experiments. (i) Pristine **1a** crystallised by vapour transport by the group of Prof. Jens Pflaum (Ref. 2a main paper) was used to deposite a film using an identical protocol to that above. Its performance was comparable to films prepared from the 95% purity **1a** prepared in Section 2 (see Table 2 main paper). (ii) A sample of the most air sensitive tetrathiotetracene **1h** (R^1, R^2 = OMe) of 88% purity (the lowest level of TTT purity used in the studies herein as determined by CHN analysis) was subjected to sublimation under conditions directly comparible to those used for film deposition. Solid **1h** (15.4 mg, 88% pure) heated to 235 °C (508 K) at 10^{-5} mbar, rapidly generating a purple band (Figure S2c) amounting to <0.05 mg. Mass spectrometry confirmed this to be 2,8-DiMeODTT [Fig. S2c, HRMS found: 350.0437 calcd. for $C_{20}H_{14}O_2S_2$, 350.0435 (dev. = +0.6 ppm)].

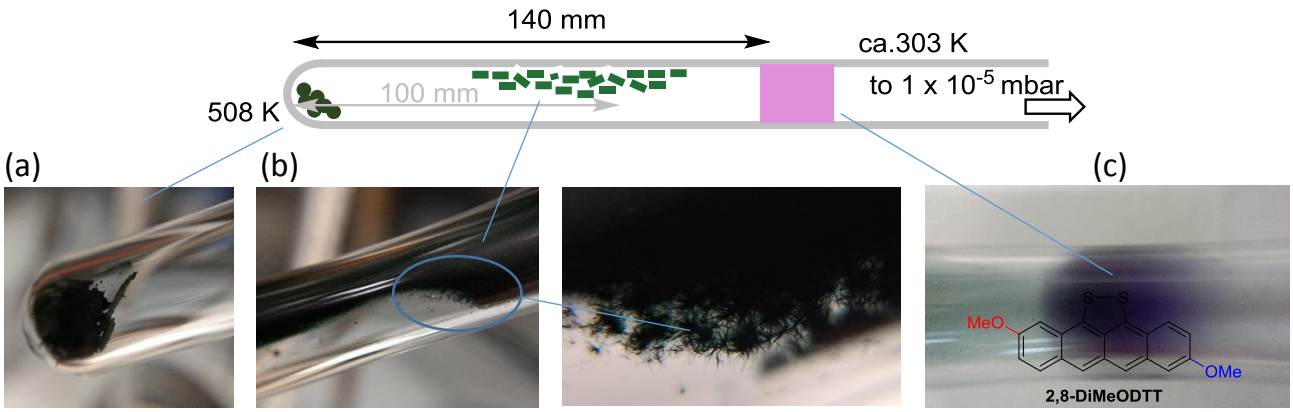

Fig S2. Apparatus used to confirm upgrade of TTT sample purity during sublimation under conditions used to generate thin film samples. (a) Non-sublimed **1h** (≤88% purity) and involatile inorganics. (b) Pure (>99%) sublimed **1h**. (c) Initially rapidly evaporated DiMeODTT (structure shown).

After 10 min a solid green band of **1h** began to develop and this continued for 1 hour giving **1h** (5.1 mg). This microcrystalline **1h** resulted showed needle like habits (up to 0.05-0.1 mm in length, Figure S2b) reminiscent of the habit observed in SEM surface studies (Figure 3; **1h**, MeO,MeO). Sublimed **1h** was ≥99% pure by CHN analysis [found C, 58.80; H, 2.91%. Calcd. for 99% pure $C_{18}H_8S_4$ C, 58.81; H, 2.96]; 500 MHz ^{1}H NMR spectroscopy [analytical sensitivity limited by the low solubility of microcrystalline TTT samples but only the expected aromatic signals for **1h** could be detected along with minor (solvent derived) impurities] and high resolution mass spectrometry [found: 411.9716 calcd. for $C_{20}H_{12}O_2S_4$, 411.9720 (dev. = -1.0 ppm) even after exposure of the samples to air for >4 h. Based on CHN analyses the purity of the residual (non-sublimed) **1h** (Fig. S2b, 10.1 mg) was degraded in purity as expected. As this sample represented the lowest purity of **1** used, for the most air sensitive sample, it was deemed that the desired enrichment of **1a-h** in all cases was attained upon bulk or film sublimation. Sublimed **1h** retained it purity for at least 4 h when handled in air. Traces of volatile purple dithiotetracene derivatives are blocked by the shutter of the experimental set-up during thin film preparation described above and not deposited in the film experiments.

SEM studies of films of **1** (using a Tescan Lyra 3 FEF-SEM × FIB with a 5 keV electron beam) are shown in Figure S3.

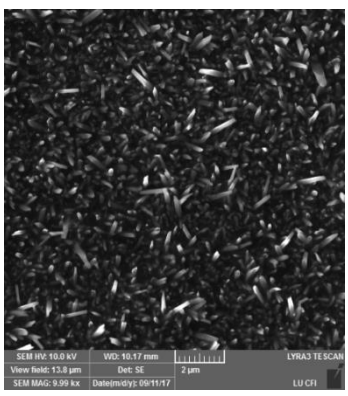

Blade habit of **1a** (TTT; H,H)

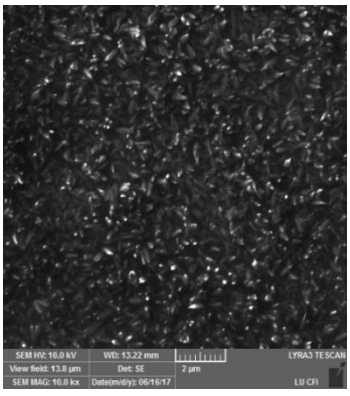

Blade habit of **1b** (Me, H)

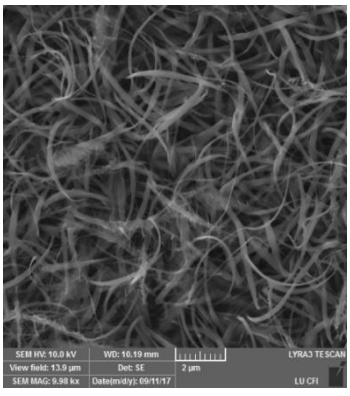

Mossy habit of **1c** (MeO, H)

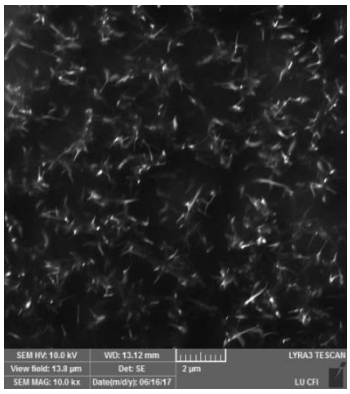

Blade habit of **1d** (Ph, H)

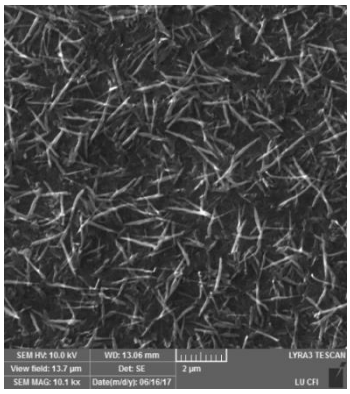

Needle habit of **1e** (Me, Me)

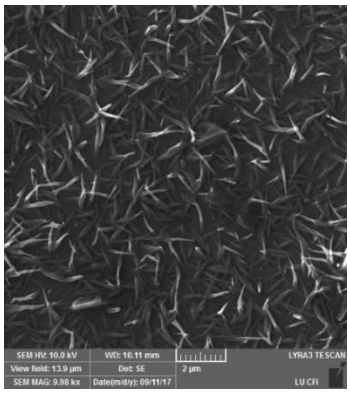

Needle habit of **1f** (*i*Pr, Me)

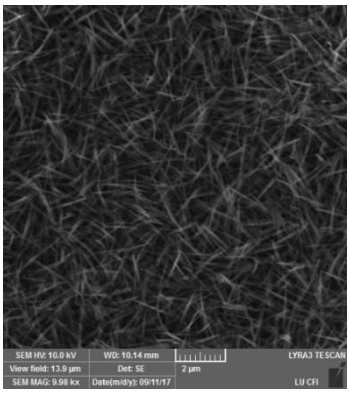

Mossy-Needle habit of **1g** (MeO, Me)

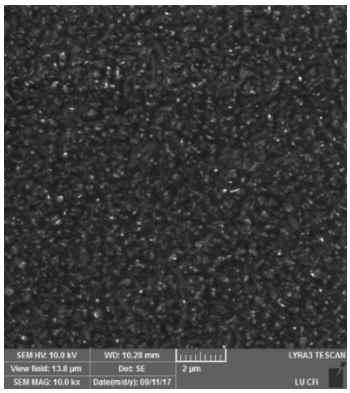

Blade habit of **1h** (MeO, MeO)

Fig S3. SEM studies of film morphologies of undoped TTT **1** derivatives.

7. Ionisation energy studies of representative un-doped thin films of 1.

In house built photoemission yield spectroscopy (PYS) system was used to determine the ionization energy of the thin films (ref. 10 main paper). The sample of **1** and a separate gold electrode above it which collected the emitted electrons were placed in the vacuum chamber. The gap between the sample of **1** and the gold electrode was ca. 2 cm. For the measurements a pressure of 1×10^{-5} mbar was used. An ENERGETIQ Laser Driven Light Source (LDLSEQ-99) was used as a light source. The wavelength (with the spectral width of 2nm) was controlled by changing the MYM-1 diffraction grating monochromator. The light/darkness cycles were switched by a Newport 76993 shutter. The sample was irradiated through a 2 × 15 mm slit in the gold electrode. A short focal length cylindrical lens was placed between the monochromator and the quartz window of the vacuum cryostat providing illumination of the 5 × 15 mm large area of the sample. A voltage (+50 V) was applied to the electrodes to collect emitted electrons. A gold electrode under the organic film of **1** precluded charging of the sample. A Keithley 617 electrometer with built in voltage source was used to apply the voltage as well as to measure the electrical current.

The photoelectron emission quantum yield spectral dependence was measured in the photon energy range from 3.50 to 6.50 eV in steps of 0.05 eV (Figure S4).

1a (4.55 eV)

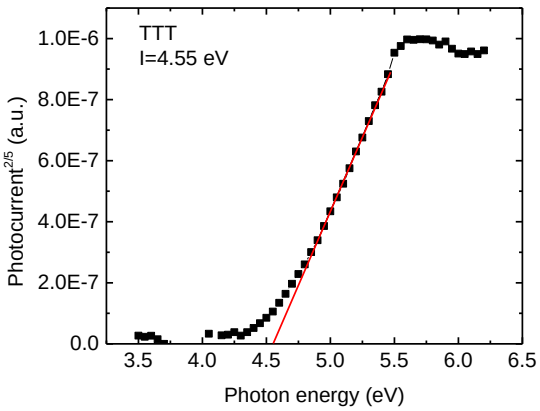

1e (4.59 eV)

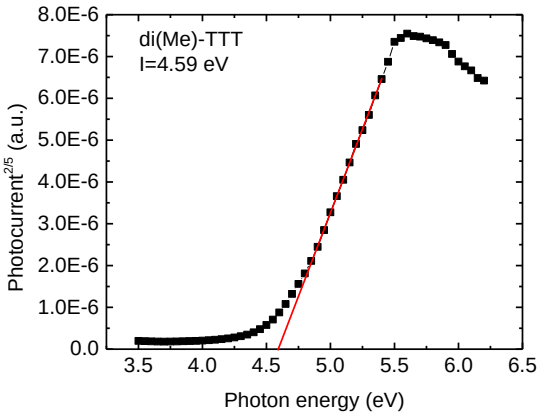

1f (4.52 eV)

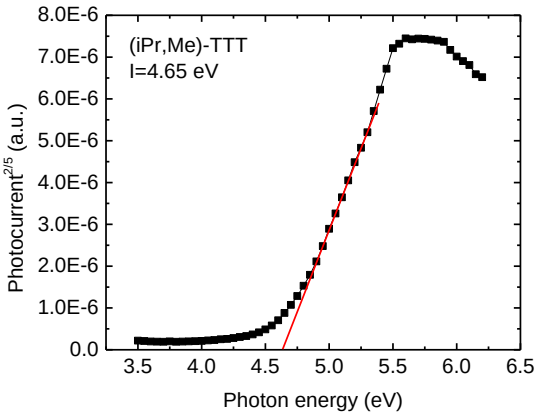

1h (4.60 eV)

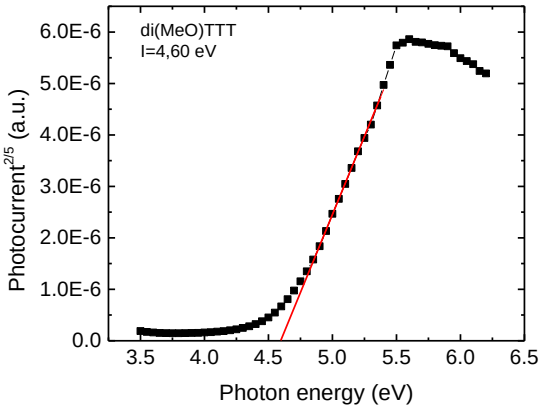

Fig. S4. Photoelectron emission determined ionisation potentials of **1a**, **1e-f**, **1h**.

The electric current difference between irradiated and non-irradiated sample was obtained. To determine the ionization energy of the studied compounds **1**, the photoemission yield *Y(hv)* was calculated as:

$$Y(h\nu) = \frac{I(h\nu)}{P(h\nu)}$$

where *I(hv)* is the number of the detected electrons and *P(hv)* is the number of the incident photons with the energy of hv. The photoemission yield can be expressed as a power law of the difference between the incident photon energy and the material ionization energy:

$$Y(h\nu) = \alpha(h\nu - E_{ioniz})^n$$

where α is constant, E_{ioniz} is ionization energy of the material and n is the number between 1 and 3 depending on the studied system.[S12] A coefficient n = 2 is usually used for metals and conductive materials[S13,S14] while n = 5/2 or n = 3 is used for semiconductors.[S15-S17] We used n = 5/2 as suggested by Kane,[S12] as it gave the best fit.

8. Iodine doped thin films of 1.

For post-deposition doping techniques thin films of **1** were treated with iodine by holding them in the chamber with a saturated iodine vapour (generated at 0.4 mbar from 99.999% I_2 – Aldrich product 229695) at 1 bar pressure at ambient temperatures (ca. 23 ^{o}C).

The iodine doping was carried out on thin films of **1** (that had already been deposited) by cyclic sample exposure to the saturated iodine vapor until the electrical conductivity measured by four contact technique ceased to rise. The cycle time varies from 1 to several minutes, depending on the increase of electrical conductivity. Such cycling technique has been chosen to reduce cracking off thin films, observed before for TTT thin films (ref. 2b main paper). The electrical conductivity in the plane of the film ($\sigma_{in\text{-}plane}$) was measured by the four probe technique using the four Au (or Cu) electrodes. A Keithley 6487 picoampermeter was used as the current source and voltage measurements were carried out by a Keithley 6514 instrument. The resultant I-V curves showed ohmic behaviour. Data from a representative run (compound **1f**), followed by electron microscope images of all resultant p-doped **1** films are shown below. Post doping with iodine the resulting TTT films were stable under ambient conditions for at least one month. SEM studies of the iodine-doped films are shown in Figure S5.

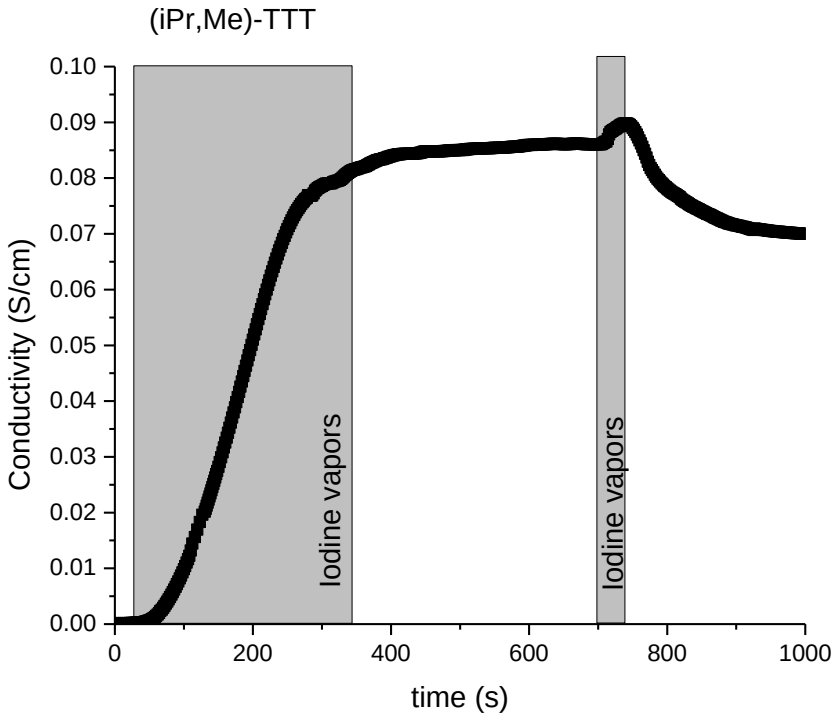

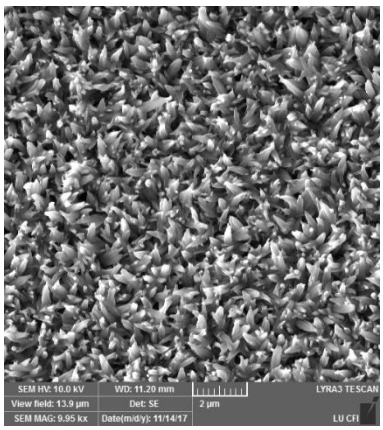

I_2 doped film **1a** (TTT; H,H)

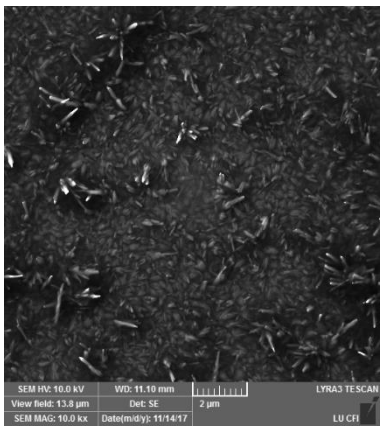

I_2 doped film **1b** (Me, H)

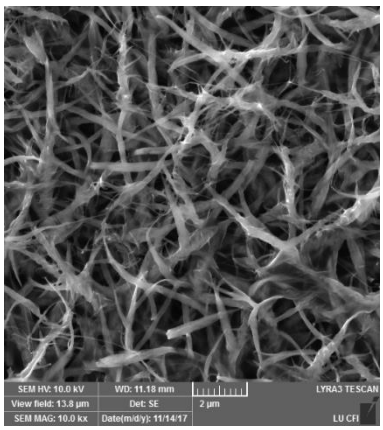

I_2 doped film **1c** (MeO, H)

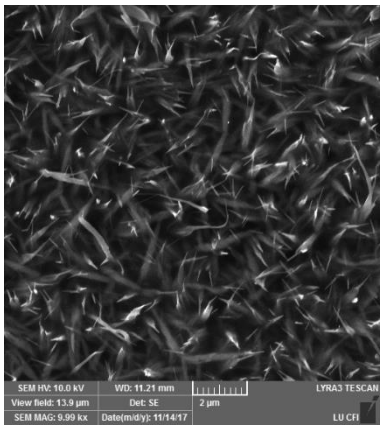

I_2 doped film **1e** (Me, Me)

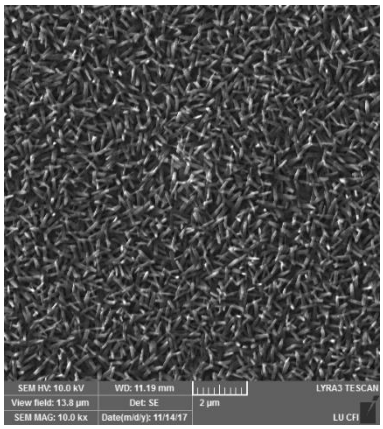

I_2 doped film **1f** (*i*Pr, Me)

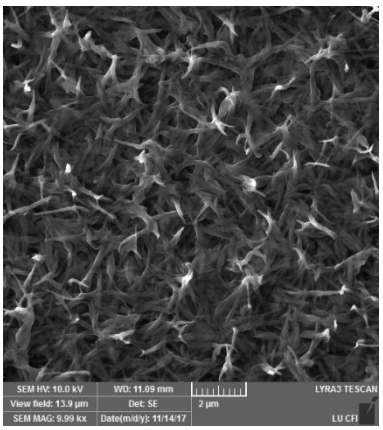

I_2 doped film **1g** (MeO, Me)

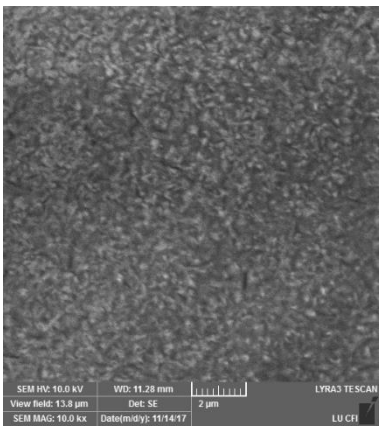

I_2 doped film **1h** (MeO, MeO)

Fig S5. Representative preparation and SEM studies of film morphologies of I_2-doped TTT **1** derivatives.

X-ray fluorescence spectroscopy studies (Figure S6) of iodine-doped **1** were carried out using EDAX/Ametek Eagle III microprobe with 40 W Rh X-ray tube at reduce pressure. Samples of **1** were attached to Erich Krause double-sided adhesive tape on teflon holder. Two types of behaviour were observed based on integration of the sulfur and iodine signals (Table S2). Films of unsubstituted **1a** and dialkyl-substituted **1e/1f** readily underdope (sulfur:iodine ratio S/I = 2.85-2.92, grey boxes), compared to the normal $TTT_2I_{3+\delta}$ ($\delta \sim 0.1$) motif, for which S/I = 2.58 is seen (in single crystalline

parent TTT **1a**) (see ref. 3 main paper). The experimentally observed stoichiometry of the **1a**, **1e** and **1f** films prepared here is rather closer to '$(TTT)_3I_{4+\delta}$' (δ = 0.1 gives S/I = 2.93 suggesting a co-crystallised mixture of $TTT_2I_{3.1}$ and TTTI). The other derivatives (**1b**, **1c**, **1d** and **1f**) are oxidised to an alternative '$TTTI_2$' stoichiometry (for which S/I = 2 is predicted; a stoichiometry not known for the parent **1a** see ref. 3 main paper, especially chapter 9). After fluorescence studies the presence of two different iodide phase was supported by ATR-IR studies on **1e** and **1h** samples (Figure S7).

Fig S6. Representative X-ray fluorescence spectra of iodine doped **1b** (S/I = 2.06), **1e** (S/I = 2.85), **1f** (S/I = 2.92), and **1h** (S/I = 1.95).

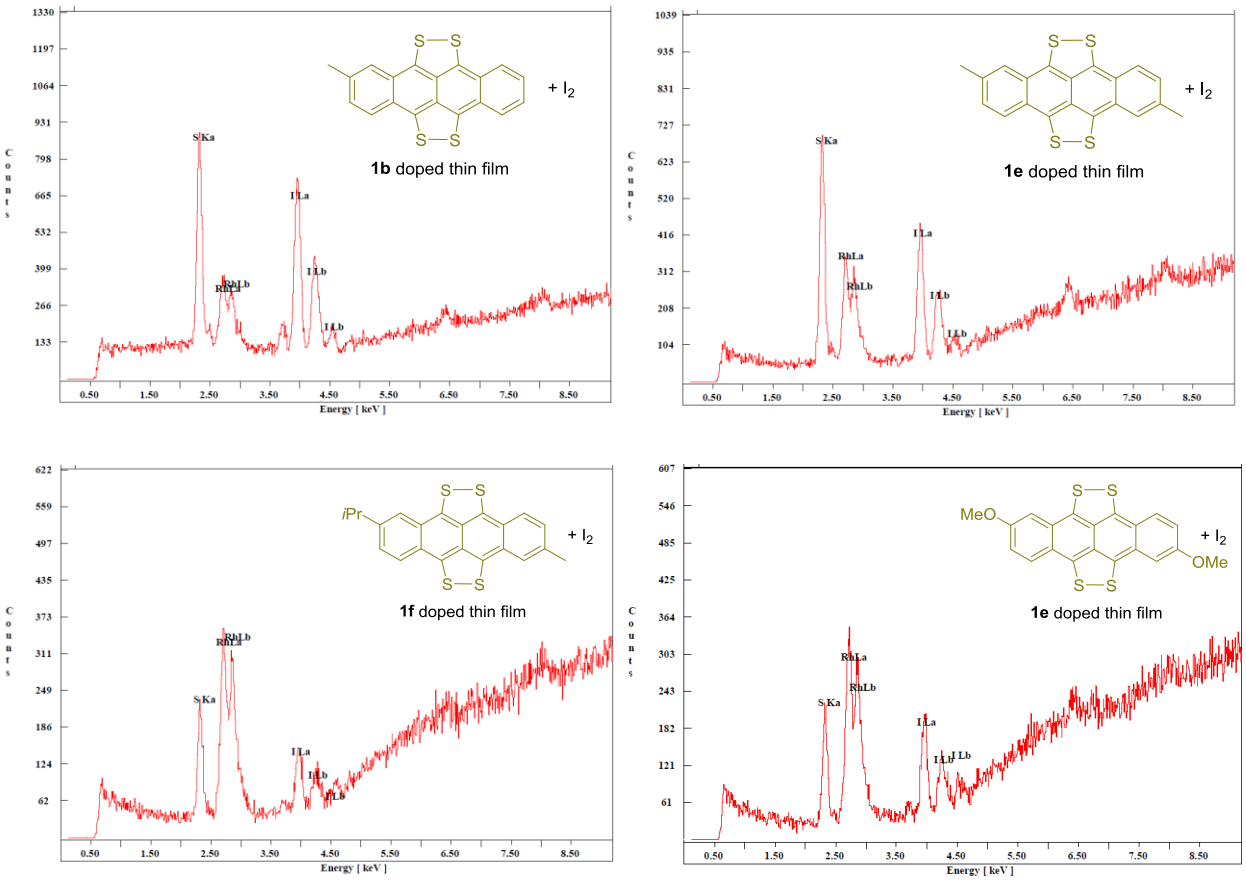

Table S2. Elemental sulfur:iodine ratio in doped films.

No.	R^1	R^2	$\sigma_{(in\text{-}plane)}$ (S cm^{-1})	S_b (μV K^{-1})	S/I ratio[a]
1a	H	H	9.52×10^{-3}	25	2.86
1b	Me	H	7.22×10^{-2}	20	2.06
1c	MeO	H	8.30×10^{-4}	17	1.95
1e	Me	Me	4.42×10^{-3}	85	2.85
1f	*i*Pr	Me	7.00×10^{-2}	216	2.92
1g	Me	MeO	2.25×10^{-2}	48	2.08
1h	MeO	MeO	6.44×10^{-3}	175	1.95

[a] Based on instrument count statistics error ±5%.

Fig. S7. IR comparison (2000-1100 cm^{-1}) of bulk and thin film **1e** and **1h** samples. Top spectra are pure pre-sublimed bulk samples in transmission, and bottom spectra (in absorbance for ease of comparison) their resultant films. In the bottom spectra green traces are pristine **1e** and **1h** and the yellow traces are films after doping treatment with I_2.

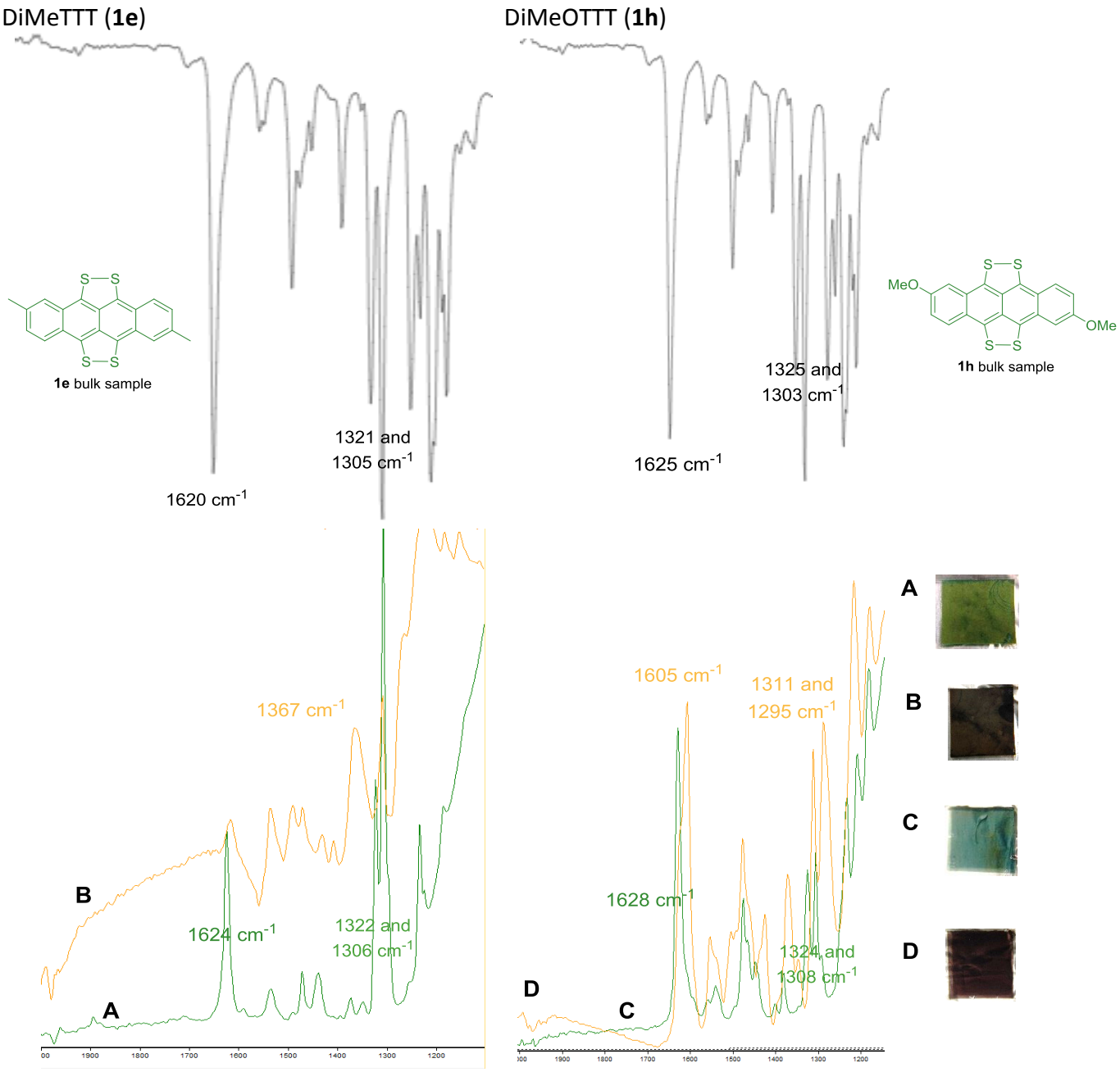

(A) DiMeTTT **1e** , (B) iodine doped DiMeTTT **1e**, (C) DiMeOTTT **1h**, (D) iodine doped DiMeOTTT **1h**.

9. X-ray photoelectron spectroscopy (XPS)

To probe the nature of the undoped and doped films XPS studies were carried out on films of **1e** (R^1,R^2 = Me) both before and after doping with I_2. Samples were analysed using the Kratos AXIS ULTRA with a mono-chromated Al kα X-ray source (1486.6 eV) operated at 10 mA emission current and 12 kV anode potential (120 W). A charge neutralizer filament was used to prevent surface charging. Hybrid–slot mode was used measuring a sample area of approximately 0.5 mm^2. The

analysis chamber pressure was better than 5 x 10^{-9} mbar. Three areas per sample were analysed. A wide scan at low resolution (1400 - -5 eV binding energy range, pass energy 80 eV, step 0.5 eV, sweep time 20 minutes) These were used to estimate the total atomic % of the detected elements. High resolution spectra at pass energy 20 eV with step of 0.1 eV, sweep times of 5 minutes (for the oxygen and carbon regions) and (10 mins (for the sulfur and iodine regions). The high resolution spectra were charge corrected to the C 1s peak set to 284.7 eV. Casaxps (version 2.3.18dev1.0x) software was used for quantification and spectral modelling. Standard Kratos calibration methods using a clean gold sample for function correction and and ag/Au/Cu peaks in the energy range were used.

Results. Analyses were carried out on a representative undoped film of **1e** (R^1,R^2 = Me) and its derived iodine doped film. A green film of **1e** (the most air sensitive of the compounds **1** prepared here), even when handled and mounted in air, showed negligible signs of aerobic oxidation either before or after doping treatment with I_2 (Figure S8). Integration revealed an extremely low oxygen content (1s signal at ca 533 eV gave 0.05-0.29 atomic %, instrument error ±0.2 atomic %). Iodine doped **1e** showed, in the S 2p region, a peak of lower sulfur binding energy (~164 eV Figure S9A) indicative of non-sulphate chemical states for which a doublet at ~168 eV or higher is expected if the sulphur became oxidised. The iodine peak in doped **1e** is very complex. It is basically a doublet (Figure S9B), but fitting of various iodine oxidation states was not diagnotsitic. This is consistent with literature obsevations on single crystals of the parent TTT_2I_3 (from **1a** R^1,R^2 = H) where the iodine chain is known to be comprised of a mixture of I^-, I_2 and I_3^- units due to the quasicrystal nature of the phase (see ref. 3 main paper). Integration of the peaks in Figure S9 was used to determine the S/I ratio (2.85±0.05).

Fig. S8. Widescan XPS spectra of **1e** (a) before doping, (b) after doping with I_2. Integration of the S and I peaks gave S/I =2.85 for the doped film of **1e**.

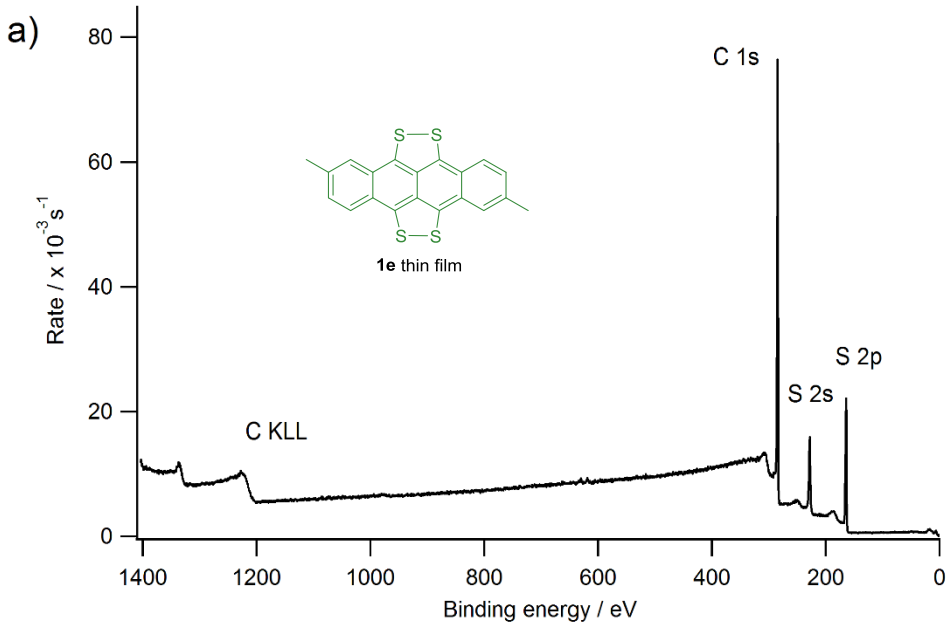

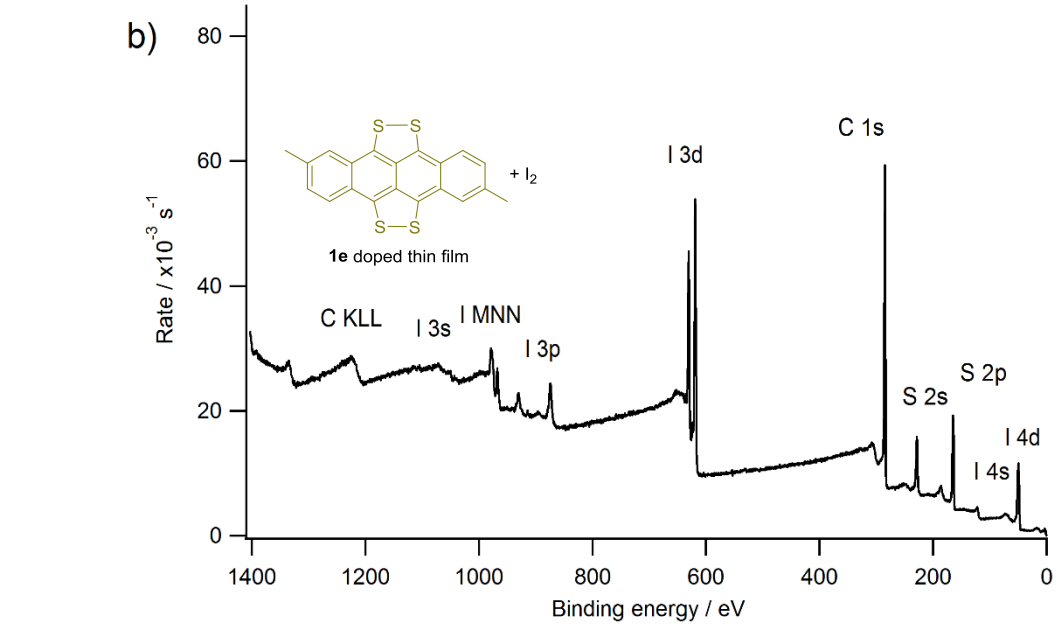

Fig. S9. Expansions of the sulfur 2p and iodine 3d peaks in iodine doped **1e**.

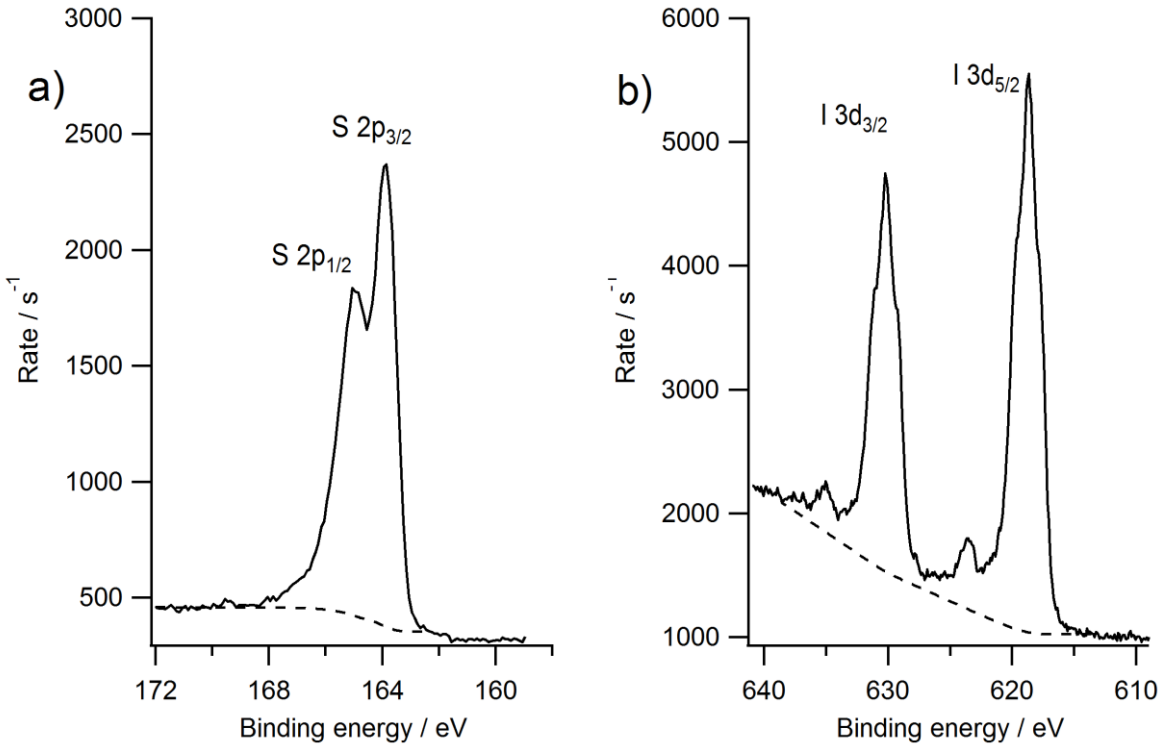

10. Calculations

The ionisation energies and electron affinities of **1a**, **1e**, **1f**, and **1h** were computed using ΔSCF methodology for calculating the energy differences between the ionic and neutral species, while keeping geometry the same (e.g. vertical excitations, as required for transport properties in the solid state).[S18] The method used for geometry optimizations and energy calculations was ωB97XD[S19] / cc-pVTZ,[S20] with CPCM (Conductor-like Polarizable Continuum Model) employed to simulate the

dielectric medium of the "self-solute" environment of **1**.[S21,S22] This model requires determination of two parameters: the optical dielectric constant (ε_e, for the fast, electronic relaxation) and the static dielectric constant (ε_s, for the slow, nuclear and molecular relaxation). Both of these constants were approximated by the Clausius–Mossotti equation (Equation S1):

$$\varepsilon = \frac{1 + \frac{8\pi}{3}\frac{\alpha}{V_m}}{1 - \frac{4\pi}{3}\frac{\alpha}{V_m}} \qquad \text{(S1)}$$

Here, V_m is the volume per single molecule, which was estimated as the molecular volume of the isodensity surface generated by Monte Carlo integration with *Gaussian 09* using 1000 points per unit area (grid density increased for improved precision). The average polarisability (α) in this equation, defined conventionally as $\alpha = \frac{1}{3}(\alpha_{xx} + \alpha_{yy} + \alpha_{zz})$, [where α_{xx}, α_{yy} and α_{zz} are diagonal elements of polarizability tensor] was either the electronic polarisability in calculations of the optical dielectric constant (ε_e), or the sum of electronic and vibrational polarisability when the equation (S1) was applied to calculate the static dielectric constant ε_s. All volumes and polarizabilities were calculated for vacuum-optimized geometries of **1**, which also served as initial structures for the "self-solute" optimizations. It was assumed that the error due to not accounting for changes in vibrations in the solid state, as well as replacement of rotations with librations ('incomplete rotations' occurring in solid state), does not exceed the error which is introduced by the rough estimation of the molecular volume. Despite its approximations this model is known to still accurately model differences between ionisation properties in vacuum and in solid state.[S22,S23] Experimental and calculated values from these studies are presented in Table S3. The difference of trend may be indicative of large influence on these molecules mutual orientation in crystals, which is obviously not accounted for by our simple solvation model. Possibley, steric interactions in solid phase of **1e** and **1f** cause the V_m to inrease substantially in comparison with that of **1a** – this explanation would fit the experimental trend.

Table S3. Measured and calculated ionisation energies and calculated electron affinity, as well as static and optical dielectric constant ε.[a]

	Measured ionisation energy (eV)	Calculated ionisation energy (eV)	Calculated electron affinity (eV)	Calculated ε_s[b]	Calculated ε_e[b]
1a	4.55	4.85	2.53	4.70	4.33
1e	4.59	4.78	2.27	4.93	4.45
1f	4.65	4.78	2.27	4.86	4.42
1h	4.60	4.69	2.30	5.43	4.23

[a] $E_g(T)$ = Ionisation energy – Electron affinity

[b] Relative permittivity vs. vacuum = 1.00.

All geometries, both vacuum and "self-solute" ones, were optimized with approximate and then the "true" force constants, confirming that the structures are true minima. Convergence thresholds, DFT grid (*FineGrid*, i.e., pruned (75,302) grid) and other parameters were left as by default.

10. References

S1. S. Woodward, M. Ackermann, S. K. Ahirwar, L. Burroughs, M. R. Garrett, J. Ritchie, J. Shine, B. Tyril, K. Simpson and P. Woodward, *Chem. Eur. J.*, 2017, **23**, 7819-7824.

S2. Available from: Mestrelab Research, S.L Feliciano Barrera 9B – Bajo, 15706 Santiago de Compostela, Spain; www.mestrelab.com

S3. The tetrathiotetracenes **1a-h** isolated in this paper show poor solubility in common NMR solvents. Carbon disulfide allowed sufficient solubility (ca. 1 mg/0.6 mL) to allow prompt collection of ^{1}H NMR data but showed minor, batch dependant, impurities [δ_H 7.01 (s), 1.12-0.98 (m), 0.83 (s), 0.70-0.51 (m), -0.21 (s)] due to the CS_2. Typically adequate signal-to-noise ^{13}C NMR spectra of **1** were acquired at 124.7 MHz after 8-16k transients with relaxation delays of 3-5 sec.

S4. Available from: Perkin-Elmer/Cambridgesoft, 940 Winter Street, Waltham, Massachusetts 02451, USA; www.cambridgesoft.com

S5. K. Pudzs, A. Vembris, J. Busenbergs, M. Rutkis and S. Woodward, *Thin Solid Films*, 2016, **598**, 214-218.

S6. K. Pudzs, A. Vembris, M. Rutkis and S. Woodward, *Adv. Electron. Mater*., 2017, **3**, 1600429.

S7. Whatman Glass Microfibre GF/A filter paper is designed for the fast filtration of fine particles (down to 1.6 µm). At larger scales this was most readily attained on 47-75 mm Hartley filter funnels with PTFE backing plates.

S8. E. A. Perez-Albuerne, H. Johnson, D. J. Trevoy, *J. Chem. Phys.*, 1971, **55**, 1547-1554.

S9. T. Nogami, H. Tanaka, S. Ohnishi, Y. Tasaka and H. Mikawa, *Bull. Chem. Soc. Jpn.*, 1984, **57**, 22-25.

S10. J. Finter, B. Hilti, C. W. Mayer, E. Minder and J. Pfeiffer, *Eur. Pat. Appl.,* 1988, EP 285564 A1, pp. 23 [*Chem. Abs*., 1989, **110**, 155481].

S11. V. Kampars and O. Neilands, *Zh. Obsh. Khim*., 1979, **49**, 2558-2560.

S12. E. O. Kane, *Phys. Rev*., 1962, **127**, 131-141.

S13. H. Monjushiro, I. Watanabe and Y. Yokoyama, *Anal. Sci*., 1991, **7**, 543-547.

S14 C. W. Ow-Yang, J. Jia, T. Aytun, M. Zamboni, A. Turak, K. Saritas and Y. Shigesato, *Thin Solid Films*, 2014, **559**, 58-63.

S15. Y. Gao, *Mater. Sci. Eng. Reports*, 2010, **68**, 39-87.

S16. M. Honda, K. Kanai, K. Komatsu, Y. Ouchi, H. Ishii, K. Seki, *Mol. Cryst. Liq. Cryst*., 2006, **455**, 219-225.

S17. K. Kanai, M. Honda, H. Ishii, Y. Ouchi and K. Seki, *Org. Electron*., 2012, **13**, 309-319.

S18. M. D. Archer, *Nanostructured and Photoelectrochemical Systems for Solar Photon Conversion*, Imperial College Press, London, 2008.

S19. J.-D. Chai and M. Head-Gordon, *Phys. Chem. Chem. Phys.*, 2008, **10**, 6615-6620.

S20. (a) T. H. Dunning, *J. Chem. Phys*., 1989, **90**, 1007-1023. (b) R. A. Kendall, T. H. Dunning and R. J. Harrison, *J. Chem. Phys*., 1992, **96**, 6796-6806. (c) D. E. Woon and T. H. Dunning, *J. Chem. Phys*., 1993, **98**, 1358-1371. (d) K. A. Peterson, D. E. Woon and T. H. Dunning, *J. Chem. Phys*., 1994, **100**, 7410-7415.

S21. A. Jurgis and M. Rutkis, unpublished work.

S22. P. E. Schwenn, P. L. Burn and B. J. Powell, *Org. Electron.*, 2011, **12**, 394-403.

S23. E. A. Silinsh, *Organic Molecular Crystals: Their Electronic States*, Springer-Verlag, 1980.